*European Journal of Taxonomy* 1064: 1–49
https://doi.org/10.5852/ejt.2026.1064.3288
europeanjournaloftaxonomy.eu
ISSN 2118-9773
2026 · Macario-González L. *et al.*


*Received: 5 May 2025* • *Accepted: 23 March 2026* • *Published: 3 June 2026*

*Topic editor: Magalie Castelin* • *Desk editor: Kristiaan Hoedemakers*

**Research article**

urn:lsid:zoobank.org:pub:6E07765C-E154-487E-AD8D-7A861E1E41A8

# Ostracodes (Crustacea: Ostracoda) from the Bacalar hydrological system, Mexico: new species with marine and freshwater affinities

Laura MACARIO-GONZÁLEZ[1], Sergio COHUO[2,*], Manuel ELÍAS-GUTIÉRREZ[3] & Héctor J. ORTIZ-LEÓN[4]

[1]Tecnológico Nacional de México / IT de la Zona Maya, Carretera Chetumal-Escárcega km 21.5, ejido Juan Sarabia, Quintana Roo 77965, México.
[2,4]Tecnológico Nacional de México / IT de Chetumal, Av. Insurgentes 330, Quintana Roo 77013, Mexico.
[3]Departamento de Ecología y Sistemática Acuática, El Colegio de la Frontera Sur, Avenida Centenario Km 5.5, Chetumal, Mexico.

[*]Corresponding author: Sergio.cd@chetumal.tecnm.mx
[1]Email: Laura.mg@zonamaya.tecnm.mx
[3]Email: melias@ecosur.mx
[4]Email: hector.ol@chetumal.tecnm.mx

**Abstract.** In this study, we examined ostracode biodiversity and species taxonomy, based on morphological characteristics, from the sulfate-bicarbonate rich, oligotrophic, and freshwater Bacalar hydrological system. A total of 19 species belonging to five subfamilies were identified. Here, we describe five new species: *Cypris nicte* Macario-González & Cohuo sp. nov., *Pseudocandona tzabek* Macario-González & Cohuo sp. nov., *Thalassocypria zazilha* Macario-González & Cohuo sp. nov., *Dolerocypria maanik* Macario-González & Cohuo sp. nov., and *Cyprideis ichkabal* Macario-González & Cohuo sp. nov. These species are clearly distinguished from their congeners by valve outline, overall shape, or appendages morphology, particularly the male sexual appendages. *Thalassocypria* Hartmann, 1957, *Dolerocypria* Tressler, 1937, *Perissocythere* Stephenson, 1938, and *Cyprideis* Jones, 1857 are distributed worldwide only in estuarine, anchialine, and marine environments. However, their continued presence in the Bacalar system at sporadically sampling for a decade suggests that the species have successfully colonized, naturalized to freshwater, and becoming established residents, likely supported by the carbonate-related high conductivity waters. We discuss the hypothetical mechanisms underlying their inland colonization and highlight the relevance of Bacalar system as a potential ecological niche supporting their freshwater establishment and distribution.

**Keywords.** Taxonomy, morphology, Yucatán Península, marine colonization.

Macario-González L., Cohuo S., Elías-Gutiérrez M. & Ortiz-León H.J. 2026. Ostracodes (Crustacea: Ostracoda) from the Bacalar hydrological system, Mexico: new species with marine and freshwater affinities. *European Journal of Taxonomy* 1064: 1–49. https://doi.org/10.5852/ejt.2026.1064.3288

## Introduction

The Bacalar hydrological system, located in the northern Neotropical region, encompasses a striking group of lakes, including Bacalar, the second largest lake in Mexico, and others with different morphometry, depth, and trophic states, ranging from mesotrophic to oligotrophic. The system is fed by groundwater flow associated with the Great Mayan aquifer. It also receives seasonal surface input from mid-elevation eutrophic water systems (~200 m a.s.l.) from the southern Yucatán Peninsula, and discharges indirectly into the Caribbean Sea (Perry *et al*. 2002, 2009).

The Bacalar system hosts one of the world's largest microbialite systems (Johnson *et al.* 2018; Yanez-Montalvo *et al.* 2020). Its geomorphology is shaped by karstic processes, including cenotes (open dolines) and fall-controlled basis that produce local sharp bathymetric gradients, with depths exceeding 40 m in some locations, even modifying environmental parameters (Perry *et al.* 2002; Bauer-Gottwein *et al.* 2011). In Cenote Azul (40 m deep), for example, a distinct water chemistry from Lake Bacalar was observed (Perry *et al.* 2002; Cervantes-Martínez *et al.* 2009), despite its geographical proximity (separated by < 80 m). Furthermore, the Bacalar system is separated from the Chetumal Bay (with estuarine conditions) by < 10 km but, to-date, marine water intrusions or biological exchange between them has not been recognized.

The biological diversity and ecological interactions in the Bacalar system have been intensively investigated during the last 20 years, motivated by both the documentation of the microbialite system (Gischler *et al.* 2008) and the potential increase of pollution attributed to urbanization, touristic infrastructure, and the increasing number of visitors (Ochoa *et al.* 2022). Currently, data about bacteria (Gischler *et al.* 2011; Johnson *et al.* 2018; Yanez-Montalvo *et al.* 2020), water mites (Montes-Ortiz & Elías-Gutiérrez 2020), nematodes (de Jesús-Navarrete *et al.* 2021; de Jesús-Navarrete & Legorreta 2022), mollusks, chironomids (Vinogradova 2008; Hamerlík *et al*. 2022), fishes (Gamboa-Pérez & Schmitter-Soto 1999; Valdez-Moreno *et al.* 2019; Uh-Navarrete *et al.* 2023), and zooplankton biodiversity (Elías-Gutiérrez *et al.* 2006, 2018; Cohuo *et al.* 2017; Macario-González *et al.* 2022) are available. The study of its biodiversity has used different approaches, from traditional taxonomy-based on morphological characters to molecular data with DNA barcoding, environmental DNA, metagenomics, and including the exploratory use of novel sampling techniques (Elías-Gutiérrez *et al.* 2018; Montes-Ortiz & Elias-Gutierrez 2018; Valdez-Moreno *et al.* 2019; Yanez-Montalvo *et al.* 2020; Uh-Navarrete *et al.* 2023). The knowledge of the biodiversity in Bacalar has advanced in terms of higher numbers of taxonomic groups being described; however, in most cases, the taxonomic identifications to species level are lacking.

Freshwater ostracodes are highly abundant in the Bacalar system, occurring in both modern environments and sedimentary records as subfossil remains (Cohuo *et al.* 2017; Mercado-Salas *et al.* 2021). Despite their abundance, taxonomical and ecological aspects of species remain poorly understood. In the northern Neotropics, ostracode species display narrow environmental tolerances (Macario-González *et al*. 2018, 2021), thereby limiting their distribution ranges and little is known about their possible exchange between marine, estuarine, and freshwater environments in coastal lakes such as the Bacalar hydrological system (Meyer *et al.* 2017).

In this study, we provide taxonomic descriptions of five new species to science, compare their diagnostic characters with closely related congeners, and discuss the relevance of the presence of marine species in the freshwater environment in Bacalar. Our findings highlight that Bacalar system is a hotspot for ostracode taxa, supporting species sympatrically coexisting with both freshwater and marine affinities.

## Material and methods

### Study area

The Bacalar hydrological system is located south in the Yucatán Peninsula, within the coordinates 18°9′ N and 18°48′ N, 88°15′ W and 88°31′ W in the Mexican state of Quintana Roo (Fig. 1). Given the nature of the karstic geology of the region, most of the waters of the Bacalar system are saturated with calcium and bicarbonates and are particularly rich in sulfates and silicates but varying between lakes (Castro-Contreras *et al.* 2014; Macario-González *et al.* 2022).

The Bacalar system consists of a series of interconnected lakes (including Bacalar and Xul-Ha), several cenotes, extensive wetlands, and the Estero de Chac, which connects the system to the Hondo River, the natural political boundary between Mexico and Belize (Fig. 1). Sediments of the hydrological system are dominated by carbonates, with calcite as the dominant mineral (Macario-González *et al.* 2022). Although a comprehensive analysis of the basin's physical dimensions and limnological characteristics

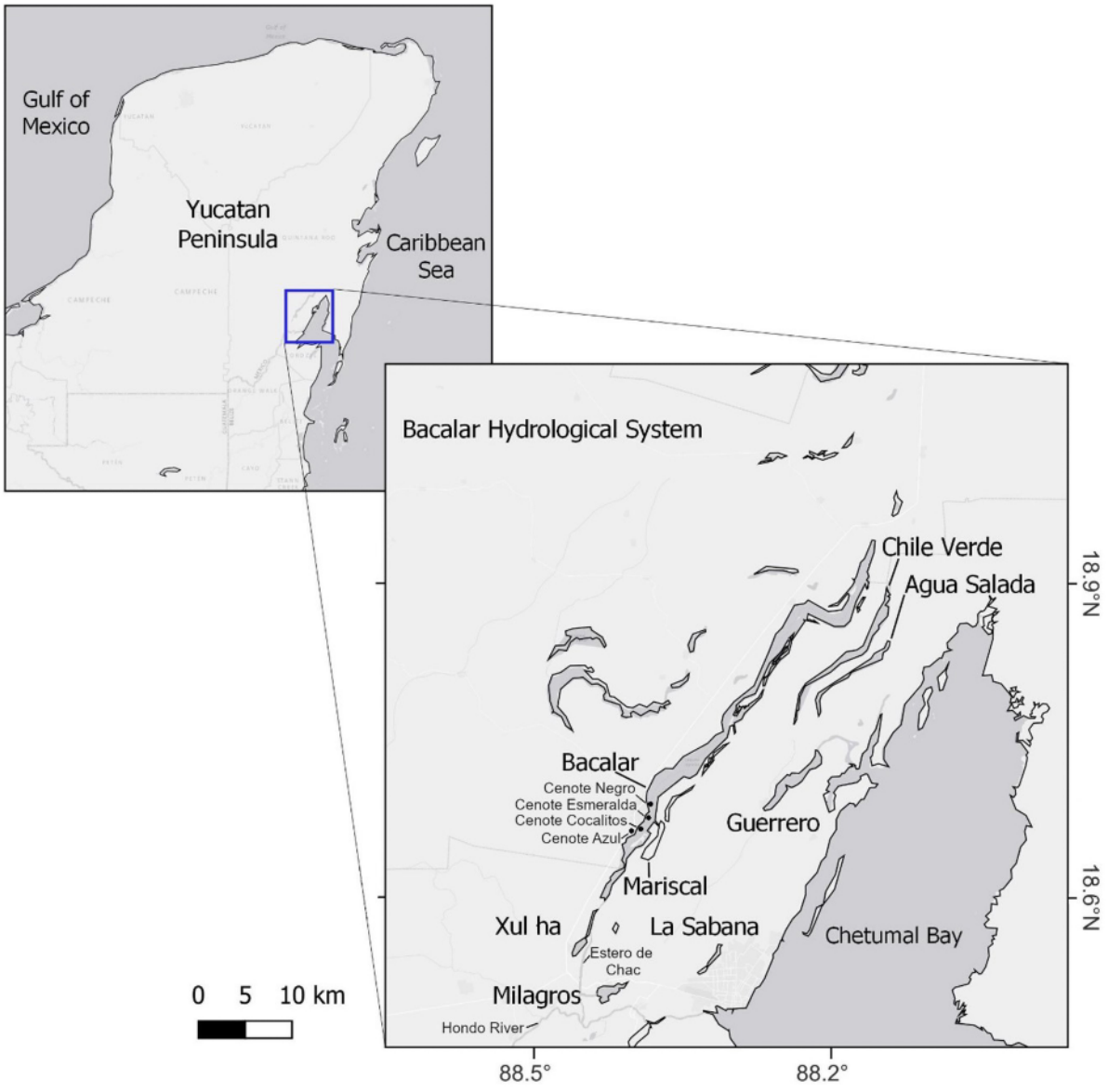


**Fig. 1.** Study area showing aquatic environments of Bacalar hydrological system.

for the entire Bacalar system is lacking, available bathymetric surveys indicate relatively shallow waters. For example, in Lake Bacalar the average depth is 8.85 m and the maximum depth is 26 m (Carrillo *et al.* 2024), while in Milagros, the maximum depth is 4.5 m. Lakes in this region are assumed to be monomictic, like the cenote Azul (Cervantes-Martínez *et al.* 2009). The region has a tropical climate (Köppen Aw), characterized by a rainy season from June to October, during which annual precipitation reaches approximately 1600 mm $y^{-1}$, and a dry season from February to May, when precipitation decreases to about 240 mm $y^{-1}$ (Macario-González *et al.* 2022). Most lakes in this hydrological system exhibit some degree of anthropogenic alterations linked to local human settlements located along their shorelines (Cohuo *et al.* 2023). In particular, the Lake Bacalar catchment is influenced by four population towns (population of ~12 000 inhabitants) (INEGI 2020), and is currently experiencing rapid population and economic growth, given the increase of touristic activities in the lake.

**Sampling and environmental variables measurements**

Five sampling campaigns were undertaken in the Bacalar hydrological system during 2010, 2013, 2015, 2019, and 2022, aiming for biological monitoring to detect early alterations in the environment and to record zooplankton biodiversity. Such campaigns were done at irregular periods of time and conducted without preference for climatic seasons.

The total number of samples varied among lakes and years and can be found in Appendix 1. A total of 26 sites were sampled in Lake Bacalar, 16 sites in Lake Xul-Ha, 14 sites in Lake Milagros, 15 sites in the Estero de Chac, 20 sites in wetlands, 21 sites in La Sabana, and 10 sites in ponds nearby. The latitude and longitude of sampling sites were determined with a Garmin GPSmap 60c and can be found in Appendix 1.

Ostracodes were collected with hand and planktonic nets of 150 µm mesh size. Since all lakes are characterized by abundant partially submerged vegetation in the littoral zone, we thoroughly sampled vegetation, rocks, and any other potential habitat. In the limnetic zone, we took vertical tows and horizontal trawls filtering approximately 200 l of water using a plankton net. Sediment samples were collected with an Ekman dredge, and the uppermost 5 cm of each sample was used to recover living organisms. All collected samples were fixed in situ with 96% ethanol and preserved on ice until final preservation at ~4°C in the laboratory. All samples were transported and processed at Instituto Tecnológico de Chetumal and El Colegio de la Frontera Sur, Chetumal Unit. For all systems, the following physical and chemical variables were measured in situ with a HACH HQ40D multiparameter probe (Appendix 2): temperature (°C), dissolved oxygen (mg $l^{-1}$), pH, and conductivity (µs $cm^{-1}$). Water depth at sampling sites were measured with a DepthTrax 1H Hawkeye.

**Ostracode assemblages**

Ostracodes were extracted and counted from a standardized volume of 50 $cm^3$ of wet sediment per sample for all littoral, water column, and sediment sites using a stereo microscope. Only organisms with complete soft parts and valves were counted. Dissection and mounting were conducted in glycerol and formaldehyde (1:1), sealed with Entellan mounting media. Shells were stored in micropaleontological slides. The appendages and valves of organisms were digitally measured and photographed with an Olympus BX41 light microscope. Appendage drawings were made from a single organism, but other individuals were observed to clarify morphological ambiguities. For drawings, we used a camera lucida attached to the same microscope and a digital drawing tablet. Non-dissected material was preserved in 96% ethanol. All material was deposited in the Zooplankton Reference Collection (ECO-CH-Z) of El Colegio de la Frontera Sur, Chetumal Unit. Species identification was based on available literature (Karanovic 2012; Cohuo *et al*. 2017) including identification keys and the original species descriptions.

Terminology of the limb chaetotaxy follows Broodbakker & Danielopol (1982), Martens (1987), and Meisch (2000), while the revised version for the second antenna and thoracopods follows Martens (1987) and Meisch (2000). Reproductive organ terminology follows Danielopol (1969, 1978). Systematics follows Meisch *et al*. (2024) and higher taxonomy of the Ostracoda follows Horne *et al*. (2002).

**List of abbreviations**

A1 = antennule
A2 = antenna
DS = distal shield
DL = distal lobe
CL = central lobe
Cp = copulatory process
GM, Gm = claws on A2
Hp = hemipenis
L5 = fifth limb
L6 = sixth limb
L7 = seventh limb
LV = left valve
Md = mandible
Mdp = mandible palp
Mxl = maxillula
Mxlp = maxilular palp
RV = right valve
UR = uropodal ramus

## Results

In the Bacalar hydrological system, 19 ostracode species belonging to the families Cyprididae (Baird, 1845), Candonidae (Kaufmann, 1900), Darwinulidae (Brady & Robertson, 1885), Limnocytheridae (Klie, 1938), and Cytheridae (Baird, 1850) were found. In Table 1, lake distribution and habitat type of each species are described.

In total, we identified six new species in the Bacalar hydrological system. Taxonomic descriptions of five of these species (*Cypris nicte* sp. nov., *Pseudocandona tzabek* sp. nov., *Thalassocypria zazilha* sp. nov., *Dolerocypria maanik* sp. nov., and *Cyprideis ichkabal* sp. nov.) are provided in the following section. *Cypria* sp. remains in open nomenclature due to insufficient material for a formal description.

**Table 1.** Freshwater ostracodes from the Bacalar hydrological system.

| Species | Lake/environment | Habitat type |
|---|---|---|
| *Cypria gibbera* | Bacalar, Cenote Azul | Littorals among vegetation |
| *Dolerocypria maanik* sp. nov. | Bacalar, Milagros, Estero Chac | Littorals without vegetation |
| *Thalassocypria zazilha* sp. nov. | Bacalar, Milagros | Water column and littorals without vegetation |
| *Paracythereis opesta* | Bacalar, Milagros, Estero Chac, Xul-Ha | Littorals without vegetation and rocky sediments |
| *Heterocypris putei* | Bacalar, Milagros | Littorals among vegetation and sediments with organic debris |
| *Cypridopsis vidua* | Bacalar, Milagros, Estero Chac, Xul-Ha, La Sabana | Water column (juveniles) and littorals among vegetation and wetlands (adults) |
| *Alicenula yucatanensis* | Xul-ha | Littorals among vegetation and wetlands |
| *Vestalenula pagliolii* | Wetlands associated with Estero Chac | Wetlands and abundant partially submerged vegetation |
| *Chlamydotheca unispinosa* | Wetlands associated with Estero Chac | Wetland and abundant partially submerged vegetation |
| *Cytheridella ilosvayi* | Bacalar, Milagros, Estero Chac, Xul-Ha, Cenote azul | Littorals with abundant vegetation and sediments with organic debris |
| *Cypria pelagica* | Bacalar, Xul-Ha | Water column and littorals among vegetation |
| *Cypria* sp. | Bacalar, Cenote Azul | Water column and littorals among vegetation |
| *Strandesia intrepida* | Bacalar, Milagros, Xul-Ha | Littorals among vegetation and sediments with organic debris |
| *Darwinula stevensonii* | Cenote Azul | Only observed in Cenote type environments associated with vegetation in the walls and littoral zone |
| *Perissocytheridea* cf. *cribrosa* | Bacalar | Rocky sediments in the littoral zone |
| *Stenocypris major* | Temporary pool | Temporary pond with partially submerged vegetation |
| *Cypris nicte* sp. nov. | Pond near La Sabana | Temporary pond with partially submerged vegetation |
| *Pseudocandona tzabek* sp. nov. | Bacalar | Littoral zone within vegetation and sediments with organic debris |
| *Cyprideis ichkabal* sp. nov. | Bacalar | Littorals without vegetation and rocky sediments |

Class Ostracoda Latreille, 1802
Subclass Podocopa G.O. Sars, 1866
Order Podocopida G.O. Sars, 1866
Suborder Cypridocopina Jones, 1901
Superfamily Cypridoidea Baird, 1845
Family Cyprididae Baird, 1845
Subfamily Cypridinae Baird, 1845
Genus *Cypris* O.F. Müller, 1776

***Cypris nicte*** Macario-González & Cohuo sp. nov.
urn:lsid:zoobank.org:act:A3C20836-EDA9-41E5-AB41-8E631C0529B6
Figs 2–5; Table 1

**Diagnosis**

Relatively big ostracodes > 1300 μm in length and > 900 μm in height. Valve L : H ratio is 0.65–0.67 and valves feature highly arched dorsal margins with greatest height at ⅖ of carapace length (Fig. 2A–D).

Shells with an anterior lip-like structure developed shortly, most prominent on RV (Figs 2E–F, 3A–B). Natatory setae of A2 exceeding the tips of the terminal claws. UR is slender with posterior claw reaching ⅔ of length of anterior claw. Genital field without projections.

**Etymology**

The epithet '*nicte*' in Mayan language means 'flower', mostly associated with *Plumeria rubra* L. and it was a common name for daughters of the Mayan K'uhul ajau (rulers of Mayan city-states) and nowadays, still the name of the Mayan princesses. The name is a noun in apposition.

**Type material**

**Holotype**

MEXICO • ♀; Quintana Roo State, Chetumal Pond, near Lake La Sabana; 18°51′ N, 88°35′ W; 7 m a.s.l.; 12 Aug. 2013; ECO-CH-Z-09319.

**Paratypes**

MEXICO • 1 ♀; Quintana Roo State, Chetumal Pond, near Lake La Sabana, 18°51′ N, 88°35′ W; 7 m a.s.l.; 12 Aug. 2013; ECO-CH-Z-12552 • 2 ♀♀; same locality as for preceding; preserved in a paleontological slide; ECO-CH-Z-12552.

**Type locality**

Ephemeral ponds near Lake La Sabana, and Chetumal city, in the federal state of Quintana Roo, Mexico (18°51′ N, 88°35′ W).

**Description**

Measurements. RV (Fig. 2A, C, E–F) measuring 1518±125 µm in average length, and 1019±132 µm in average height (n=4). The LV (Figs 2B, D, 3A–B) is 1540±95 µm in average length and 1075±105 µm in average height (n=4).

**Female** (holotype)

Carapace. In lateral view subtriangular-shaped (Fig. 2A–D). The LV is slightly larger than the RV, both anteriorly and posteriorly, except in the lip-like projection area (Fig. 2E–F). Shell in dorsal margin is highly arched, displaying the greatest height around ⅖ of the shell. The anterior margins with the selvage inwardly displaced forming a well-developed flange (lip-like projection) round and shortly developed (Fig. 2E–F); the posterior margin is broadly rounded. The ventral margin is almost straight, except in the mouth region, where it is slightly concave. The RV (Fig. 2A, C, E–F) measures 1580 µm in length, and 1105 µm in height. Calcified inner lamella is narrow, anteriorly equaling 12.6% and posteriorly 5.6% of the total length of the shell (Fig. 2E–F). The LV (Figs 2B, D, 3A–B) is 1602 µm in length and 1145 µm in height. The calcified inner lamella is narrow, the anterior and posterior lamellae are equal to 10.7% and 4.3% of the total length of the shell, respectively (Fig. 3A–B). The anterior marginal pore canals are straight and denser than in the posterior region. Muscle scars consist of four compact scars and two more antero-ventrally elongated scars. The surface of the shell is punctate and sparsely covered by "Porenwarzen" (Fig. 3C). Hinge adont.

A1 (Fig. 4A). 7-segmented. First segment with one antero-medial seta and two postero-distal setae. Second segment has one smooth apical seta anteriorly. Rome's organ is represented by a small projection. The third segment carries two short, smooth setae, with the anterior one slightly longer than the posterior one. Fourth segment with two elongated, hairy setae anteriorly, equaling 11 times as long as the terminal segment, plus a small seta just exceeding the distal end of following segment. Posteriorly two smooth setae of unequal length. The fifth segment anteriorly carries two long and hairy setae, 14.2 times as long as the terminal segment, and two subequal, smooth posterior setae. Sixth segment has four long apical,

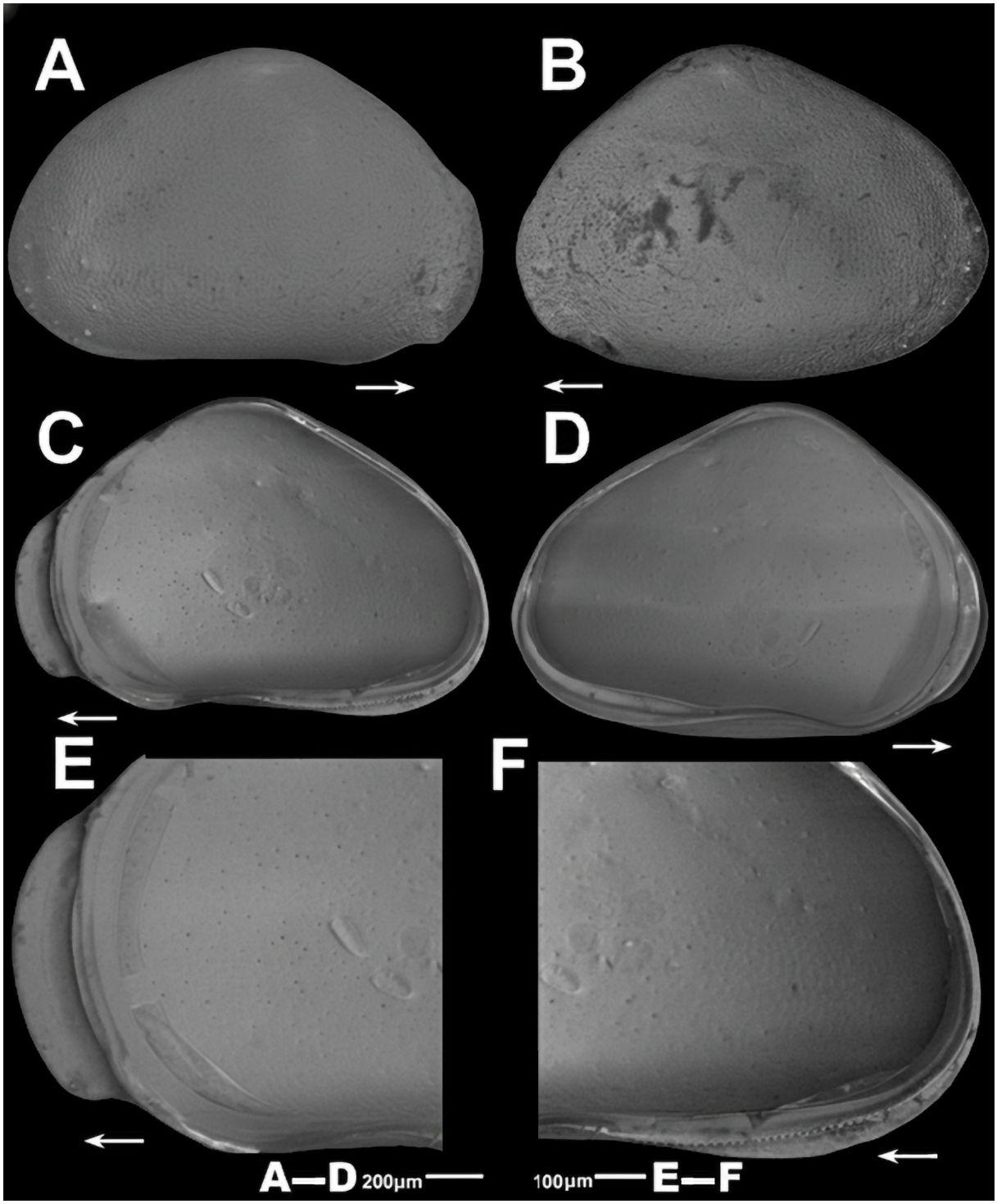


**Fig. 2.** *Cypris nicte* Macario-González & Cohuo sp. nov., holotype, ♀ (ECO-CH-Z-09319). SEM analysis. **A, C**. Right valve, external and internal views, respectively. **B, D**. Left valve, external and internal views, respectively. **E**. Anterior part of right valve. **F**. Posterior part of right valve. White arrows show the valve orientation toward the anterior margin.

hairy setae of unequal length, plus a small seta that just exceeds the distal end of terminal segment. The longest is 13.5 times as long as the terminal segment. Seventh (terminal) segment has two long, hairy distal setae and one short, smooth seta. Aesthetasc (ya) is 3.2 times as long as the terminal segment. Length ratios of the last five segments are 2.6 : 0.9 : 1 : 0.9 : 1.

A2 (Fig. 4B). 5-segmented. Coxa carries three relatively long and smooth setae. Basis with one seta that does not reach the distal end of the following segment. Exopod consists of a plate with three unequally long setae; the longest one just exceeding the distal end of following segment. First endopodal segment (I) hirsute. Aesthetasc Y is 1.6 times as long as terminal segment, which postero-distally displays one long and serrulate seta widened at the base and reaching the distal end of the terminal segment. Natatory setae consist of a row of five long and hairy setae extended beyond the tip of the terminal claws and one short and smooth seta located more anteriorly. Second endopodal segment (II) slightly hirsute and carrying antero-medially two unequally long and smooth setae. Postero-medially with the four t-setae present; the "t1" seta is claw-like developed and the "t4" seta is very small. All z-setae (z1–z3) do not reach the tip of the terminal claws. G1 claw is slightly smaller and thinner than the adjacent claws. G2

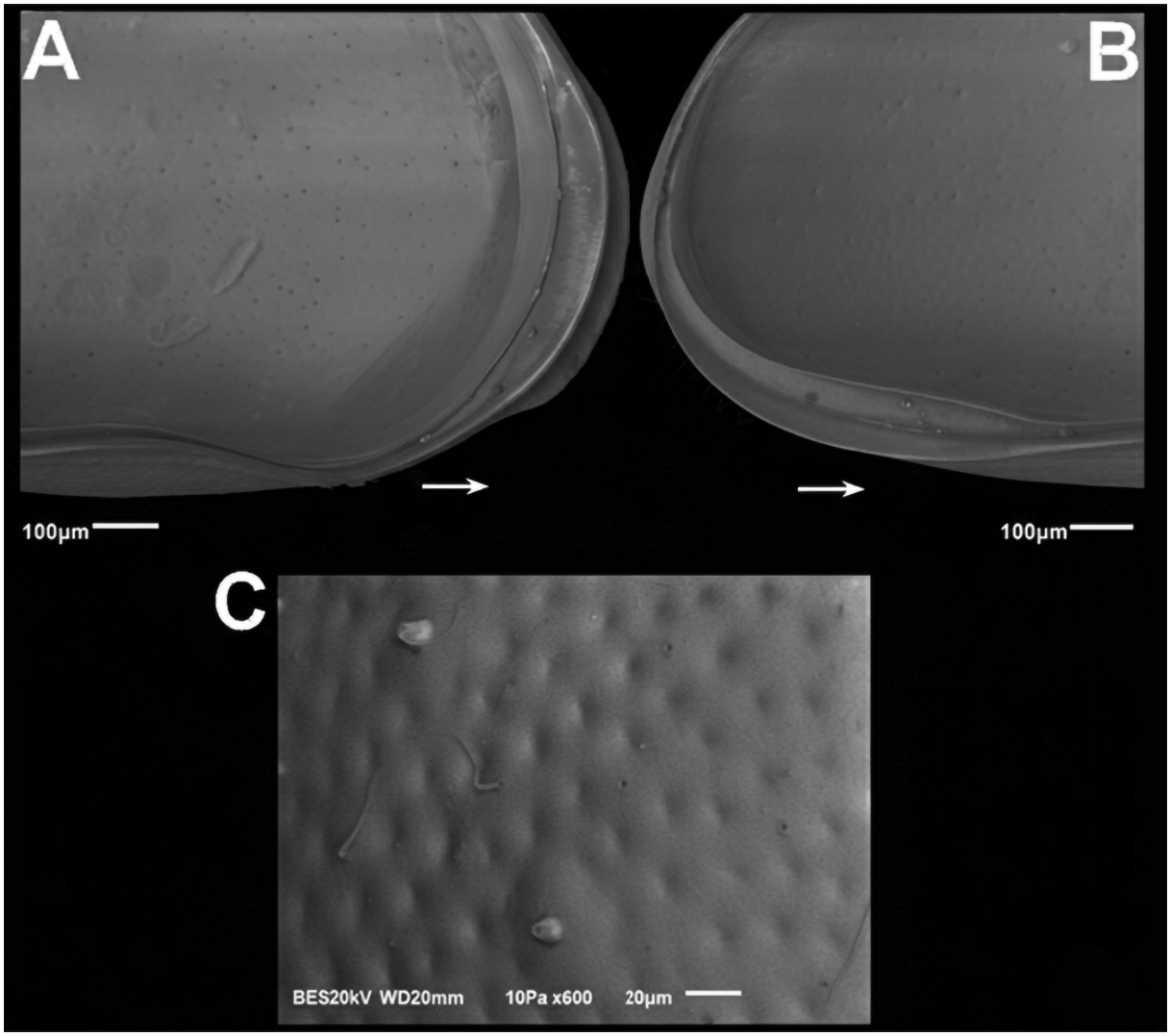


**Fig. 3.** *Cypris nicte* Macario-González & Cohuo sp. nov., holotype, ♀ (ECO-CH-Z-09319). SEM analysis. **A**. Anterior part of left valve. **B**. Posterior part of left valve. **C**. Close-up of valve surface showing "Porenwarzen". White arrows show the valve orientation toward the anterior margin.

and G3 are strongly serrated in the ⅔ distally, and subequally long; 5.2 times as long as terminal segment. Third endopodal segment (III) with a thin GM claw, equaling 4.8 times as long as the terminal segment (Fig. 4B'). Gm short and serrulate distally. Aesthetasc y2 is thin and 1.1 times as long as terminal segment (Fig. 4B').

Md and Mdp (Fig. 4C). The coxa consists of a plate with a row of nine pointed teeth and one short and smooth seta. Mdp 4-segmented. First segment ventrally with S1 and S2 setae long and plumose. Setae α, thin and small, reach the distal end of the following segment. The second segment with three unequally long setae dorso-distally and ventro-distally with four setae, longest seta plumose and exceeding distal end of the terminal segment. Seta β is short and hairy. Third segment is hirsute and distally with twelve

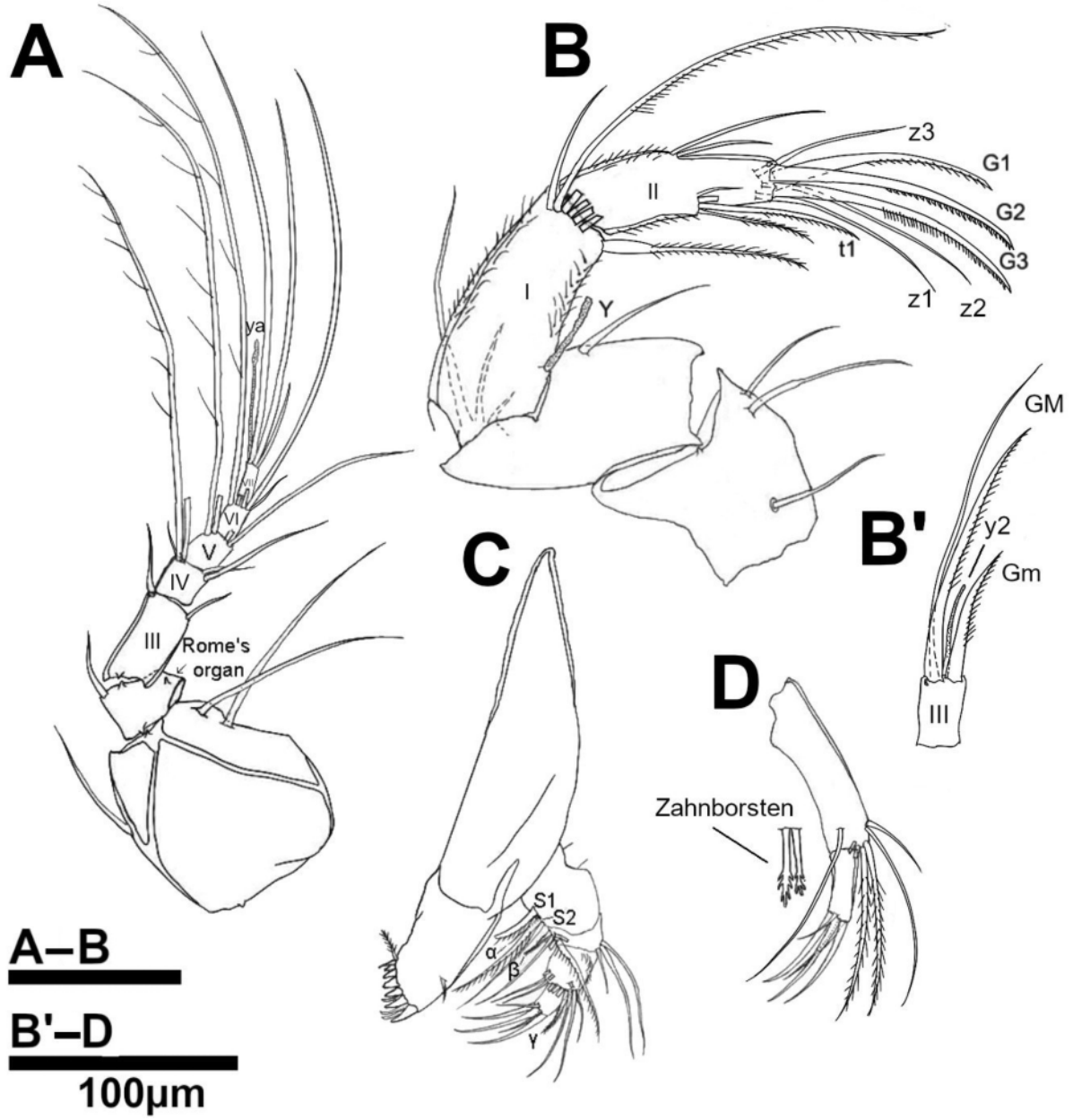


**Fig. 4.** *Cypris nicte* Macario-González & Cohuo sp. nov., holotype, ♀ (ECO-CH-Z-09319). **A**. A1. **B**. A2. **B'**. Third endopodal segment of A2. **C**. Md and Mdp. **D**. Mxl and "Zahnborsten".

unequally long setae. Seta γ widened at the base and distally hairy. Fourth segment (terminal) with three claw-like and two slender setae.

MXLP (Fig. 4D). Palp 2-segmented. The first segment displays seven apical and unequally long setae. The second segment is rectangular, with the distal end carrying three claw-like and two short and slender setae. Third endite displays two long, strong and serrated "Zahnborsten".

L5 (Fig. 5A). The protopodite hirsute on one side with eleven sub-equally long and serrulate setae. Two setae are present: seta b serrulate and seta d smooth. Endopodite with three unequally long and serrulate setae. Respiratory plate with six plumose rays.

L6 (Fig. 5B). 4-segmented. Basal segment with two unequally long setae (d1 and d2). Second segment hirsute on dorsal and ventral sides with one short and serrulate e-seta distally. Third segment with a long

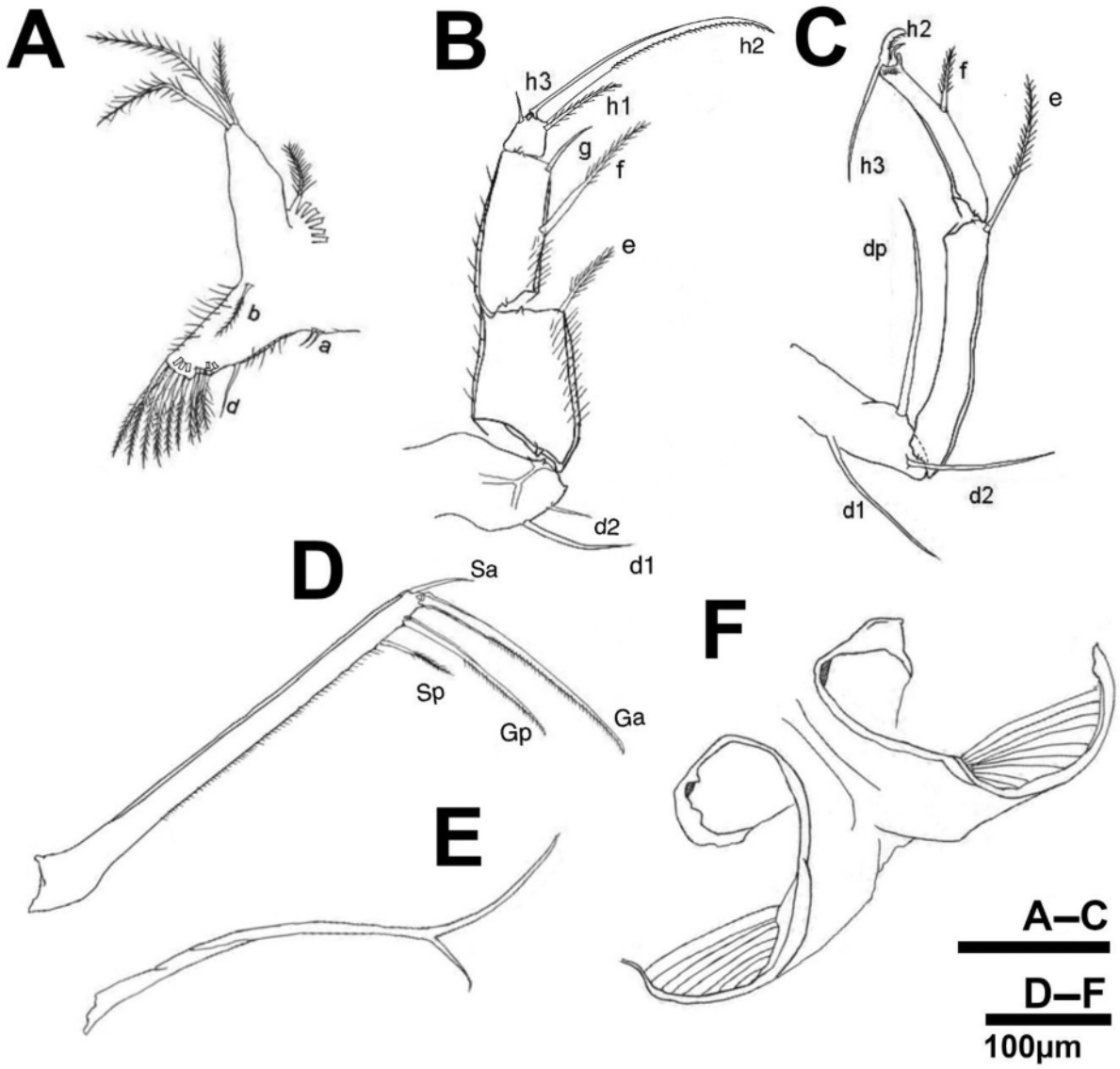


**Fig. 5.** *Cypris nicte* Macario-González & Cohuo sp. nov., holotype, ♀ (ECO-CH-Z-09319). **A**. L5. **B**. L6. **C**. L7. **D**. UR. **E**. UR attachment. **F**. Female sexual field.

and serrulate f-seta and a short and smooth g-seta. Fourth segment with a long and hirsute h1 seta and a short and smooth h3 seta. Claw (h2) slightly distally curved and serrated, equaling 7.2 times as long as the terminal segment.

L7 (Fig. 5C). 4-segmented. Basal segment with d1, d2 and dp setae present. First endopodal segment with a serrulate and long e-setae exceeding the half-length of the following segment. Third endopodal segment with hirsute and short f-setae. Terminal segment with smooth and elongated h3 setae. Seta h2 is claw-like and curved; h1 seta is transformed into a pincer organ.

UR (Fig. 5D). Ramus elongated and robust with the posterior margin hirsute. Anterior claw distally hairy and exceeding half the length of the ramus. The anterior seta is small and smooth. Posterior claw is distally hairy and reaching ⅔ of the length of the anterior claw. Posterior seta serrulate, just reaching the distal end of the ramus. The UR attachment is elongated and distally bifurcated (Fig. 5E). Sexual field with no posterior projections or lobes, but with radial structures in the outer parts of field (Fig. 5F), with ovaries inwardly displaced (not drawn).

**Differential diagnosis**

*Cypris nicte* sp. nov. is most closely related to *C. decaryi* Gauthier, 1933 and *C. pretusi* Mesquita-Joanes *et al*. 2020, as all three species share relatively smooth valve surfaces, lack spine-like structures on the valves, and possess a well-developed lip-like projection on the RV. However, *Cypris nicte* differs from *C. pretusi* primarily in valve length: the new species is approximately 1.6 mm, whereas *C. pretusi* ranges from 1.7 to 2 mm (Mesquita-Joanes *et al*. 2020). *Cypris pretusi* has postero-ventrally a row of pointed denticles, absent in *Cypris nicte*. Although *Cypris decaryi* is a relatively common and cosmopolitan species, detailed morphological descriptions of its soft parts are lacking, and its carapace shape and size exhibit considerable regional variability. As in the case with many other "cosmopolitan" ostracode species, *C. decaryi* likely represents a species complex. In African populations, Martens (1990) reported a length range of 1.4–1.8 mm and a height range of 1.2–1.3 mm. Consequently, the L : H ratio of 0.69–0.77 is used as a taxonomic character. *Cypris nicte* falls within the length and height range of *C. decaryi*, but differs in its L : W ratio, which is 0.65–0.67. The greatest height of the carapace in *C. nicte* is located at 2/5 of the carapace length, whereas in *C. decaryi*, it is situated at mid-length (½ of the valve). Neale (1976) noted that the natatory setae on A2 in *C. decaryi* do not exceed the distal end of terminal claws, while in *C. nicte*, they at least reach the tips or exceed the terminal claws. Likewise, the posterior claw (Gp) on the UR in *C. decaryi* does not reach half the length of the anterior claw, whereas in *C. nicte*, the posterior claw (Gp) extends ⅔ of the anterior claw's (Ga) length (Fig. 5D).

**Remarks**

The genus *Cypris* has a worldwide distribution with about 18 species, most of them present in a single biogeographical region, mainly in the Palearctic and Afrotropical. Still, species such as *C. decaryi* Gauthier, 1933, *C. granulata* Daday, 1898, and *C. pubera* O.F. Müller, 1776 are cosmopolites (Mesquita-Joanes *et al*. 2020; Meisch *et al*. 2024). In the Neotropical region, only these three cosmopolitan species have been recorded, and in Mexico, uncertain records of *C. mexicana* Ehrenberg, 1869 (currently no valid species name) and *C. granulata* under the name *C. subglobosa* Sowerby, 1840 fide Meisch *et al*. 2019, have been reported so far (Machain-Castillo & Gío-Argáez 1993). *Cypris nicte* sp. nov. in the timeframe of a decade has been observed once in temporary ponds, suggesting that it may not be a resident in the Bacalar hydrological system, but instead seasonally introduced by either wind transport of resting eggs (Rosa *et al.* 2023), mammal or reptile dispersion (Tomowski *et al.* 2025) or similar mechanisms. The large size and pigmentation of this species in oligotrophic environments may be ecologically disadvantageous for them, as individuals may be more visible in comparison to other ostracodes inhabiting the environment and thus facilitate predation. The presence of only female individuals in the population suggests that this species reproduces parthenogenetically, supporting its capacity to rapidly colonize newly formed environments. We additionally observed some juvenile specimens (likely A3–A1 instars), all of them with strongly serrated, posterior margins. This indicates that the species exhibits distinct ontogenic variation in shell morphology. Environmental conditions of the sampled pond were as follows: temperature 32°C, dissolved oxygen 7 mg $l^{-1}$, pH 8.6, conductivity 1001 µS $cm^{-1}$.

Family Candonidae Kaufmann, 1900
Subfamily Candoninae Kaufmann, 1900
Genus *Pseudocandona* Sars, 1923

***Pseudocandona tzabek*** Macario-González & Cohuo sp. nov.
urn:lsid:zoobank.org:act:EDCC8AA9-E514-42BB-8DF0-8F95D62E4D80
Figs 6–9, Table 1

**Diagnosis**

Carapace is subtrapezoidal, with a straight dorsal margin. Shell surface is smooth. LV overlaps RV anteriorly and posteriorly. Mdp with a setae group consisting of 4+1 setae. L5 with setae a, b, and d present. L6 with all apical setae short. Female sexual field with a small, digitiform projection. Male prehensile palps are robust and globose. Hemipenis with all lobes approximately equal in length; lobe "h" broadly rounded. The ejaculatory process is distally curved and pointed.

**Etymology**

The name of this species was proposed by Juan Manuel Salazar Montes, a biology student from the Instituto Tecnólogico de Chetumal, as part of a local contest to name the species. In the Mayan language, this word means "group of stars" and is mainly associated with the Pleiades constellation. This name must be treated as a noun in apposition.

**Material examined**

**Holotype**
MEXICO • ♂; Quintana Roo State, Lake Chacchoben; 19°03′ N, 88°18′ W; 4 m a.s.l.; 12 Aug. 2013; ECO-CH-Z-09323.

**Allotype**
MEXICO • ♀; Quintana Roo State, Lake Chacchoben; 19°03′ N, 88°18′ W; 4 m a.s.l.; 12 Aug. 2013; ECO-CH-Z-09324.

**Paratypes**
MEXICO • 2 ♂♂, 3 ♀♀; Quintana Roo State, Corozo Pond; 19°27′ N, 88°52′ W; 20 m a.s.l.; 25 Aug. 2013; plastic tube with 70% ethanol; ECO-CH-Z-09324.

**Type locality**

Partially submerged vegetation in littoral of Lake Chacchoben (19°03′ N, 88°18′ W), located in the federal state of Quintana Roo, Mexico.

**Description**

Measurements. Males: the RV (Fig. 6A) is 788.89±95 µm in average length and 394.93±78 µm in average height (n=3). The LV (Fig. 6B) is 832.8±88 µm in average length and 414.47±83 µm average height (n=3). Females: RV (Fig. 6C) is 749.32±75 µm in average length and 359.88±56 µm in average height (n=7). LV (Fig. 6D) is 776.81±68 µm in average length and 373.44±66 µm average height (n=7).

**Male** (holotype)
Carapace. In lateral view subtrapezoidal (Fig. 6A–B). LV is larger than RV anteriorly and posteriorly. Dorsal margin almost straight. Greatest height around ¾ of shell length. Anterior and posterior margins are rounded, with the anterior narrower than the posterior. Ventral margin slightly concave around middle; posteriorly slightly downwardly projected. Right valve (Fig. 6A) 732.5 µm in length and 377.3 µm in height. Calcified inner lamella covering 13.6% anteriorly and 4.3% posteriorly of the total shell length. Left valve (Fig. 6B) 765.7 µm in length and 395.2 µm height. Calcified inner lamella anteriorly and posteriorly covering 15.3% and 5.6% of total shell length, respectively. Marginal pore canals are straight

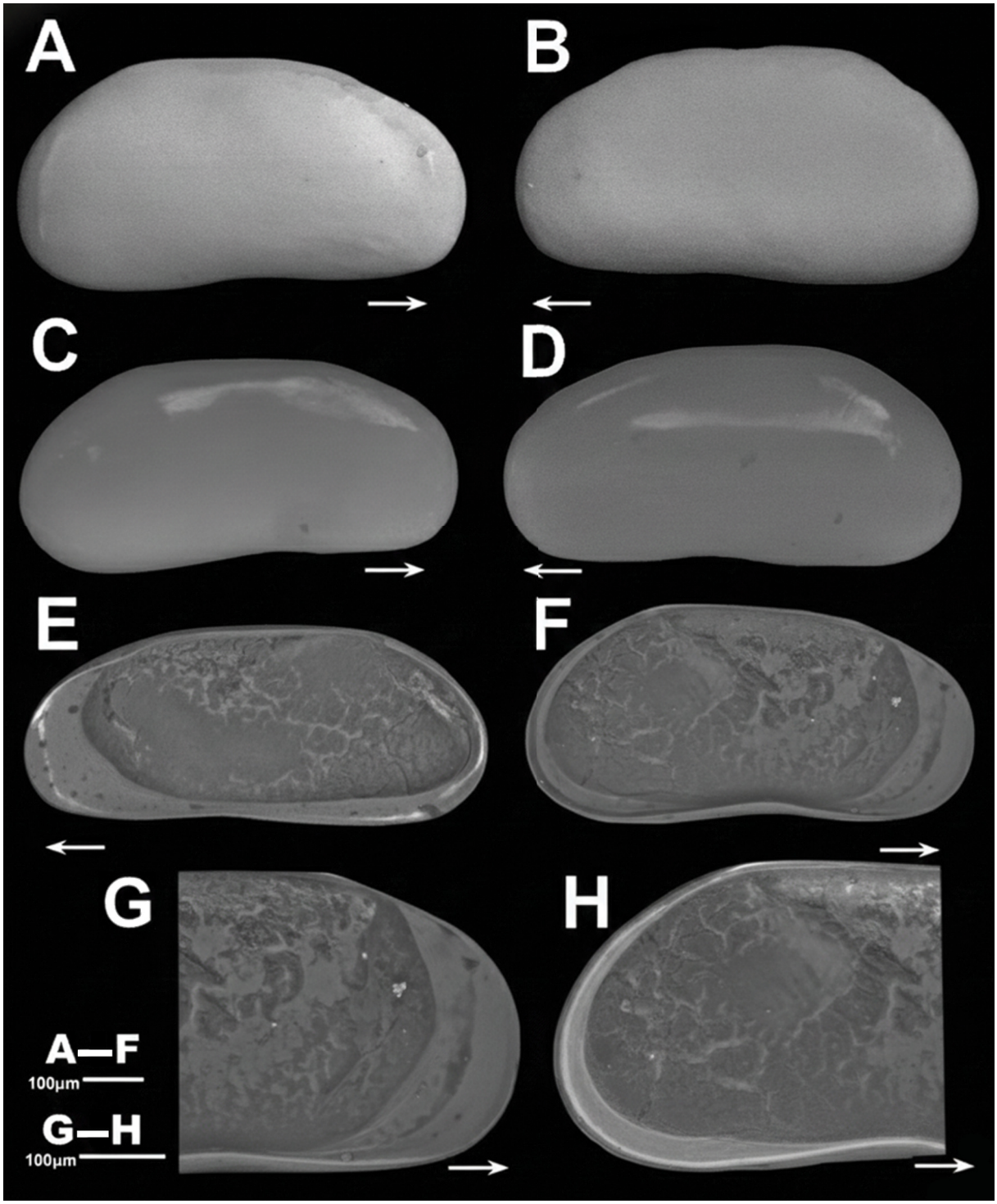


**Fig. 6.** *Pseudocandona tzabek* Macario-González & Cohuo sp. nov., holotype, ♂ (ECO-CH-Z-09323) and allotype, ♀ (ECO-CH-Z-09324). **A–B**. ♂, right and left valves, external view, respectively. **C–D**. ♀, external views of right and left valves, respectively. **E–F**. ♀, internal views of right and left valves, respectively. **G–H**. ♀, close-up of left valve anterior and posterior internal margin, respectively. White arrows show the valve orientation toward the anterior margin.

and scarce. Selvage peripheral. Muscle scars are composed of four central scars and two elongated scars antero-ventrally. Shell surface is smooth. Hinge adont.

A1 (Fig. 7A). 6-segmented. First segment with two postero-distally serrulate setae, longer one reaching distal end of antepenultimate segments. Anteriorly on the same segment one proximal serrulate seta and one smooth and short seta distally. Second segment anteriorly with one apical smooth seta. The third segment (III) carries one short seta medially and three setae apically, of which the anterior ones long, exceeding by far the distal end of the last segment. Fourth segment (IV) with two elongated setae anteriorly and one short seta posteriorly. Fifth segment (V) with three setae, the most anteriorly located are elongated and by far exceeding the distal end of the last segment. Terminal segment (VI) distally with two long and one short setae. Aesthetasc (ya) 1.6 times as long as the terminal segment. Length ratios of the last 5 segments are as follows: 1.2 : 1.8 : 1 : 1.3 : 1.

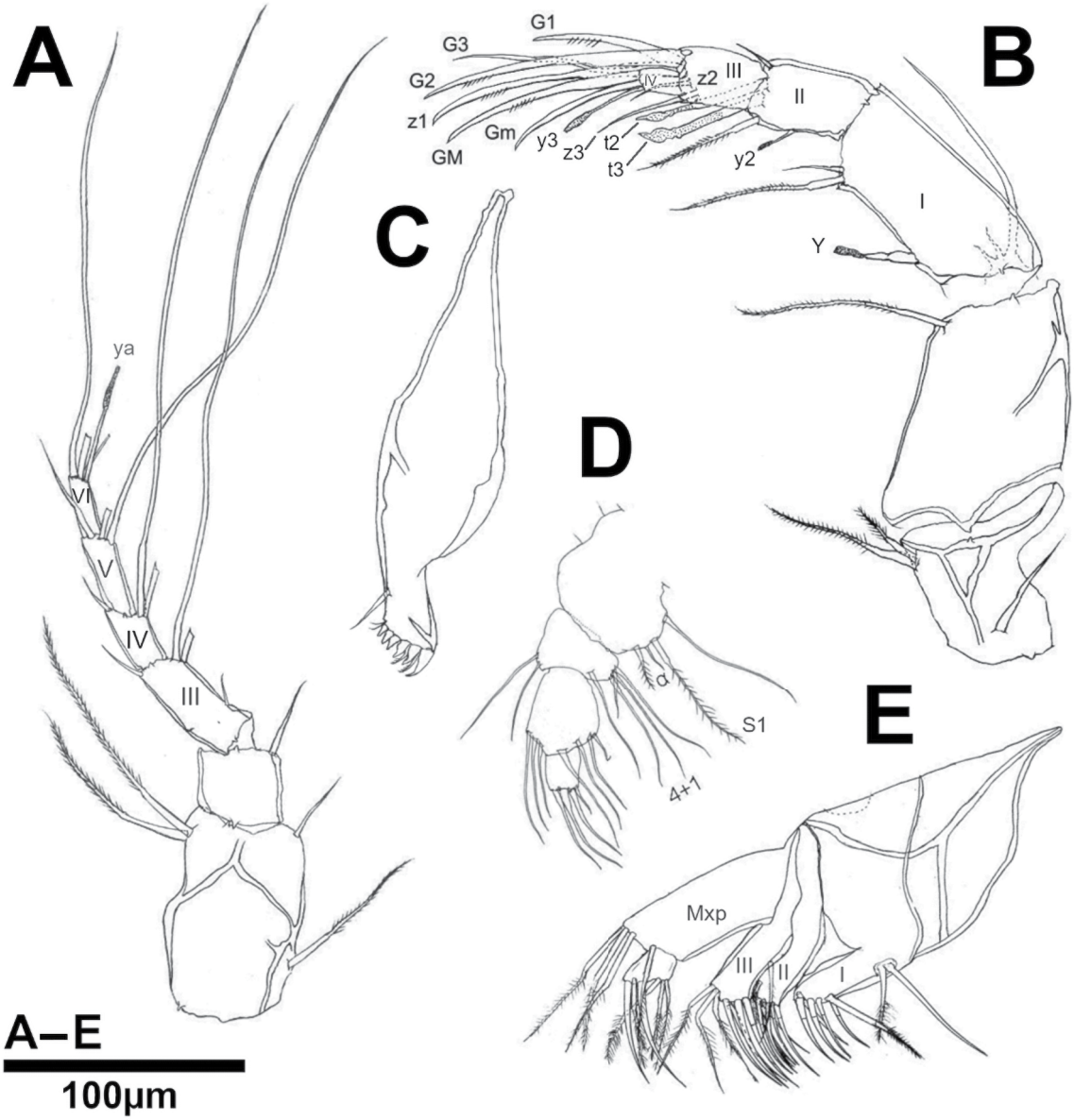


**Fig. 7.** *Pseudocandona tzabek* Macario-González & Cohuo sp. nov., holotype, ♂ (ECO-CH-Z-09323). **A**. A1. **B**. A2. **C**. Md. **D**. Mdp. **E**. Mxl and Mxlp.

A2 (Fig. 7B). 6-segmented. Coxa with two postero-distally serrulate setae and one smooth seta, basally located. Basis with one long and serrulate seta not reaching the distal end of the following segment. Exopod consists of a plate with three unequally long setae, longer seta just exceeds the distal end of the following segment. First endopodal segment (I) with aesthetasc Y, 2.2 times as long as the terminal segment. Postero-distally on this same segment two unequally long setae. Second endopodal segment with aesthetasc y2 thin, 1.1 times as long as terminal segment. Antero-distally on this segment one short seta, and postero-distally one serrulate seta. Sexual bristles (t2, t3) elongated ending with a semi-triangular structure. Third endopodal segment with setae z2, z3, short and thin. Seta z1 transformed into a claw. Apically on this same segment, the claw G1 is short, 3.1 times as long as the terminal segment and G2 is elongated, 5.2 times as long as terminal segment. G3 is transformed into a seta. Terminal segment is carrying a GM claw-like and Gm transformed into a strong seta. Aesthetasc y3 thin and 2 times as long as terminal segment.

Md and Mdp. Coxa (Fig. 7C) consists of a plate ending with a row of eight pointed teeth and one short and smooth seta. Mdp 4-segmented (Fig. 7D). First segment ventrally with four setae; seta S1 long and plumose. Seta located most proximally, smooth, with the same length as S1. Seta α, thin and small. Second segment dorsally with two setae. Ventrally 4+1 setae. Third segment dorso-distally with three bare and unequally long setae. Ventro-distally of this same segment four smooth and unequal setae; three exceeding the distal end of the last segment. Fourth segment (terminal segment) with four smooth setae; three of them subequally long, 2.8 times as long as terminal segment.

Mxl and Mxlp (Fig. 7E). Mxl with four endites with variable number of setae almost of the same length. First endite (I) basally with two long setae and distally with six setae, longer one serrulate. Second endite (II) with seven setae distally, all of them smooth and of approximate same length. Third endite (III) with seven setae distally, three of them serrulate. An additional serrulate seta is located basally on this endite. Mxlp 2-segmented. First segment carries three apical and serrulate setae and one central seta. Second segment squarish and distally with six setae; four are serrulate, while the other two are smooth.

L5 (Fig. 8A). Protopodite apically with twelve unequally long and smooth or plumose setae. Prehensile palps asymmetrical; right one with a globose finger and left one robust and distally curved. Both palps with two thin subapical seta-like structures. Setae a, b, and d present.

L6 (Fig. 8B). 5-segmented. Basal segment with only d1 setae. First, second, and third endopodal segments all carry one apical short seta (e, f, g, respectively. Terminal segment with two distal thin and small setae, representing h1 and h3. Claw (h2) is curved and slightly serrated distally; its length equals 4.8. times as long as the terminal segment.

L7 (Fig. 8C). Basal segment with d1, d2 and dp setae. Second segment bare. Third segment with long and serrulate g-seta. Terminal segment with h2 and h3 seta elongated; seta h1 shorter than adjacent one.

UR and attachment (Fig. 8D–E). Ramus slender and hirsute along posterior margin. Terminal claws are slightly curved distally and serrulate. Ga-claw exceeding half the length of the ramus. Sa-seta small. Gp-claw almost equaling the length of anterior one. Sp-seta serrulate and not reaching the distal end of the ramus. The UR attachment is distally bifurcated (Fig. 8E).

Hemipenis (Fig. 8F). With a robust body; “a” lobe digitiform with the base slightly widened. Lobe b not well sclerotized, with distal margin rounded and medially positioned. Lobe h with distal margin broadly rounded; 1.3 times as wide as lobe b. Ejaculatory process (e) pointed and distally slightly curved. The M-process is distally triangular-shaped. Internal canals double coiled. Zenker’s organ elongated with 7 whorl of spines (not drawn).

**Female** (allotype)

CARAPACE. The carapace is slightly smaller than that of the males. Valve surface is smooth (Fig. 6C–D). LV overlaps RV anteriorly and posteriorly. RV (Fig. 6C) is 728.8 µm in length and 335.8 µm in height. Inner lamella covering 5.5% anteriorly and 4.76 posteriorly of valve length (Fig. 6E). LV (Fig. 6D) is 720.6 µm in length and 342.5 µm in height. Inner lamella covering 15% anteriorly and 5.9 posteriorly of valve length (Fig. 6F–H). Hinge adont.

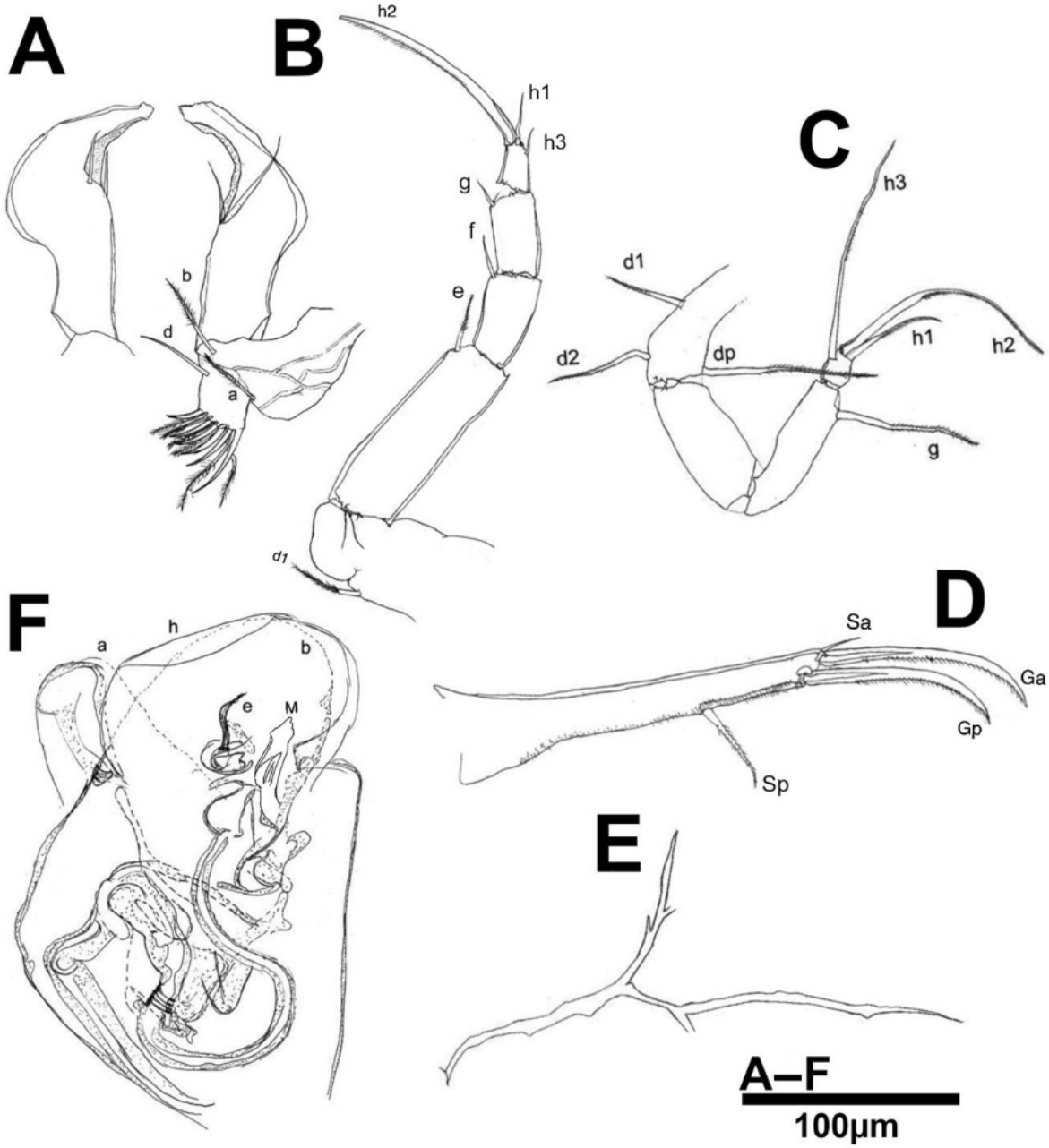


**Fig. 8.** *Pseudocandona tzabek* Macario-González & Cohuo sp. nov., holotype, ♂ (ECO-CH-Z-09323). **A**. Right prehensile palp and L5 with palp. **B**. L6. **C**. L7. **D**. UR. **E**. UR attachment. **F**. Hemipenis.

A1 (Fig. 9A). Almost equally as in males; third and fourth segments are fused. Middle seta on third segment missing. Antero-apical setae shorter than in males. Sixth segment (VI) with one thin and small additional seta.

A2 (Fig. 9B). Sexually dimorphic. 5-segmented, the second and third endopodal segments in males are fused in females. Second endopodal segment with all t-setae. Setae z1 and z2 are short; seta z3 is elongated, measuring 2.3 times as long as the terminal segment. Claw G2 is reduced, 1.8 times as long as

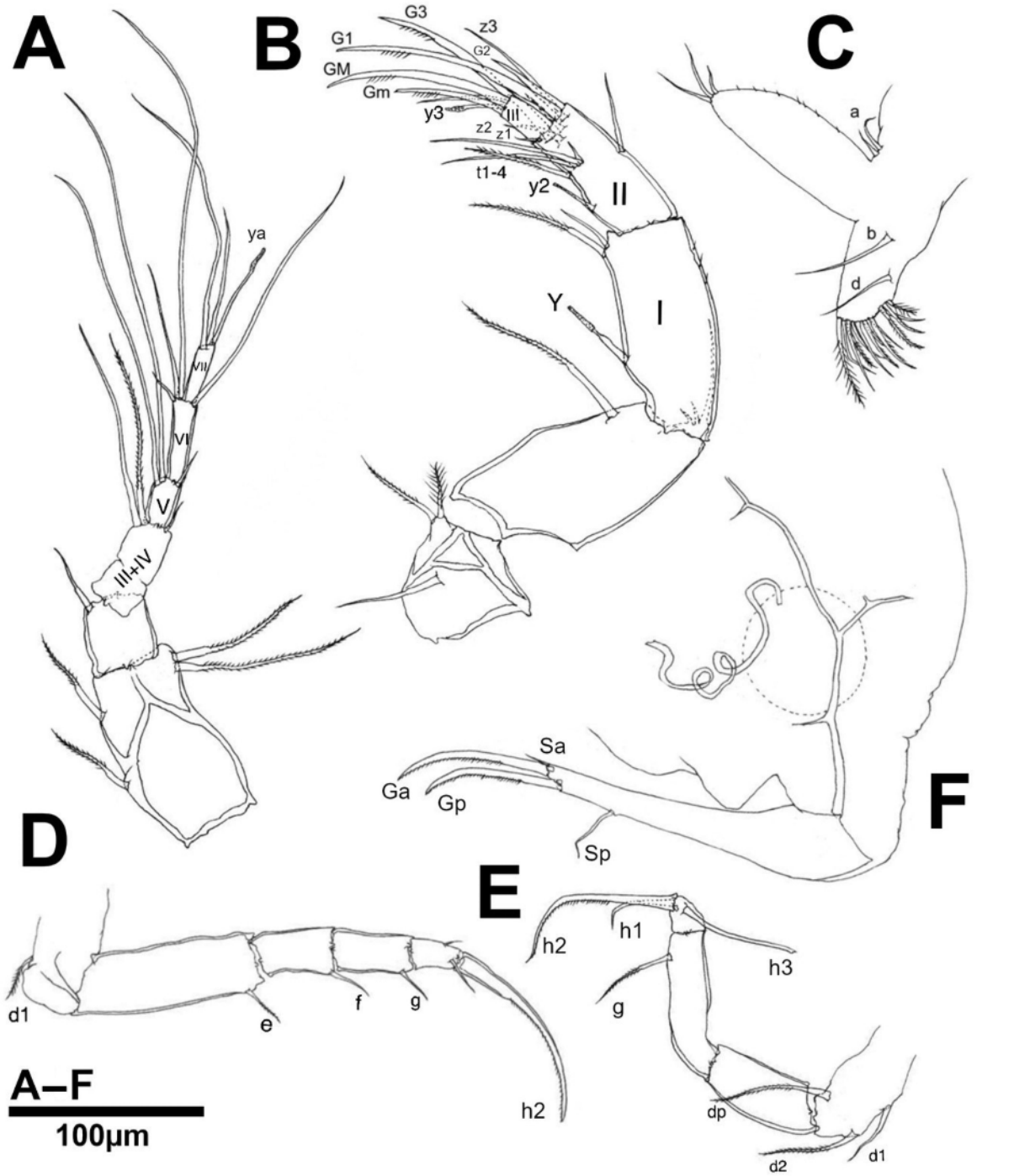


**Fig. 9.** *Pseudocandona tzabek* Macario-González & Cohuo sp. nov., allotype, ♀ (ECO-CH-Z-09324). **A**. A1. **B**. A2. **C**. L5. **D**. L6. **E**. L7. **F**. UR and sexual field.

the terminal segment. Claws G1 and G3 are subequal in length, 4.4 times as long as the terminal segment. Claws GM and Gm measure 3.2 and 2.1 times as long as the terminal segment, respectively.

Md, Mdp, and Mxlp. As in males.

L5 (Fig. 9C). With fourteen smooth or serrulate setae on distal end of protopodite. Endopodite is slightly hirsute with three short setae distally. Two a, and one b and d setae present.

L6 (Fig. 9D) and L7 (Fig. 9E). Similar as in males. In female's L7, however, dp seta is slightly shorter than in males. This seta does not exceed the distal end of the following segment, whereas it does in males.

UR (Fig. 9F). With anterior (Ga) and posterior (Gp) claw almost equally long, just reaching the middle of the ramus. Ramus is not hirsute as in males. The genital field (Fig. 9F) displays a small triangular projection.

**Differential diagnosis**

Based on its morphology, *Pseudocandona tzabek* sp. nov. belongs to the *caribbeana*-group because of the presence of 4+1 setae in the second segment of the Mdp, the h1 seta on the L7 is long and elongated but not hook-like, and because the A2 has six segments, with G2, Gm and z1 as claws in males. Within this group, *P. caribbeana* Broodbakker, 1983, *P. cubensis* Broodbakker, 1983, *P. claudinae* Higuti & Martens, 2014, and *P. elliptica* Furtos, 1933 are the closest relatives to *P. tzabek* because of shell characteristics and similarities of the male sexual appendages. *Pseudocandona caribbeana* and *P. cubensis* however, are distinct from *P. tzabek* as they display a reticulation with pits across the shell surface (Broodbakker 1983), whereas *P. tzabek* has a smooth shell surface (Fig. 6A–D). The A1 is 8-segmented in *P. caribbeana* and *P. cubensis*, whereas 6-segmented in *P. tzabek*. The distal seta on the penultimate segment of L6 by far overpasses the distal end of the terminal segment in *P. caribbeana* and *P. cubensis*, but it is short and does not reach half-length of terminal segment in *P. tzabek*. Additionally, *P. caribbeana* lacks the triangular projection on the female sexual field as observed in *P. tzabek*. Although *Pseudocandona claudinae* has a similar shell morphology, females are slightly smaller (length 693 µm and height 348 µm) than those of *P. tzabek* (749 µm length and 359 µm height) and their carapace has a slightly rounded dorsal margin, whereas almost flat in the new species. Other appendage differences between them are A1 7-segmented, the very short e-seta on the L6 and the elongated f-seta overpassing the distal end of the terminal segment in *P. claudinae*. In addition, the UR is stout with relatively short terminal claws; all these characteristics are contrary to *P. tzabek*. *Pseudocandona elliptica* differs mainly in shell morphology, because this species is reniform; however, the soft part morphology, and in particular the hemipenis, is very similar to that of *P. tzabek*. This structure only differs in a lobe extension, which is projected slightly beyond lobes b and h, while in *P. tzabek* the three lobes have approximately the same extension. The prehensile palps are slightly different as well, with the fingers slender and elongated in *P. elliptica* and globose and slightly compressed in *P. tzabek*.

**Remarks**

*Pseudocandona tzabek* sp. nov. was found inhabiting lakes, open cenotes (not caves), and wetlands, always associated with the littoral zone or among submerged vegetation. This species is relatively broadly distributed on the southern Yucatán Peninsula. Average environmental conditions at the sampling site: temperature 33.1°C, dissolved oxygen 9.4 mg $l^{-1}$, pH 9.9, conductivity 1241 µS $cm^{-1}$.

Subfamily Thalassocypridinae Hartmann & Puri, 1974
Genus *Thalassocypria* Hartmann, 1957

***Thalassocypria zazilha*** Macario-González & Cohuo sp. nov.
urn:lsid:zoobank.org:act:96979B89-D9AB-420B-A7B9-6F945713D22C
Figs 10–13, Table 1

**Diagnosis**

Relatively small animals (< 700 μm) with almost reniform valve shape. Valve anteriorly broadly rounded and posteriorly narrow, slightly downwardly projected; antero-dorsally with a small depression, more visible in males. Male specimens are slightly smaller than females. Rome's organ elongated and distally widened. On A2, natatory setae by far exceeding the tips of terminal claw. The male prehensile palps are almost symmetrical; the right one displays a constriction at the middle of the finger. The hemipenis is small with the outer and inner lobes broadly rounded; medial lobe slightly pointed.

**Etymology**

Zazil-ha is a Mayan word that means "transparent waters" and refers to the type of environment in which this species lives, being the oligotrophic waters in the Bacalar hydrological system. This name was proposed by Cinthia Yahaira Balam Chable, a biology student from the Instituto Tecnológico de Chetumal, as part of a local contest to name the species. This name must be treated as a noun in apposition.

**Type material**

**Holotype**

MEXICO • ♂; Quintana Roo State, Lake Bacalar; 18°70′ N, 88°38′ W; 0.4 m a.s.l.; 20 Oct. 2024; ECO-CH-Z-09320.

**Allotype**

MEXICO • ♀; Quintana Roo State, Lake Bacalar; 18°70′ N, 88°38′ W; 0.4 m a.s.l.; 20 Oct. 2024; ECO-CH-Z-09321.

**Paratypes**

MEXICO • 2 ♂♂; Lake Milagros 18°51′ N, 88°42′ W; 6 m a.s.l.; 20 Oct. 2024; soft parts dissected in slides and valves preserved in paleontological slides; ECO-CH-Z-12551, ECO-CH-Z-12554 • 2 ♀♀; same collection data as for preceding; soft parts dissected in slides and valves preserved in paleontological slides; ECO-CH-Z-09322, ECO-CH-Z-12554.

**Localities**

Partially submerged vegetation and water column of Lake Milagros (18°51′ N, 88°42′ W), next to the community of Huay Pix, Quintana Roo Federal State, Mexico. Other sites where the species has been observed, Lake Bacalar.

**Description**

Measurements. Males: RV (Fig. 10A) is 585.76±88 μm in average length and 272.82±92 μm in average height (n=3). LV (Fig. 10B) is 592.54±85 μm in average length and 285.97±87 μm in average height (n=3). Females: RV (Fig. 10C) is 644.16±86 μm in average length and 300.45±88 μm in average height (n=3). LV (Fig. 10D) is 682.44±91 μm in average length and 302.3±92 μm in average height (n=3).

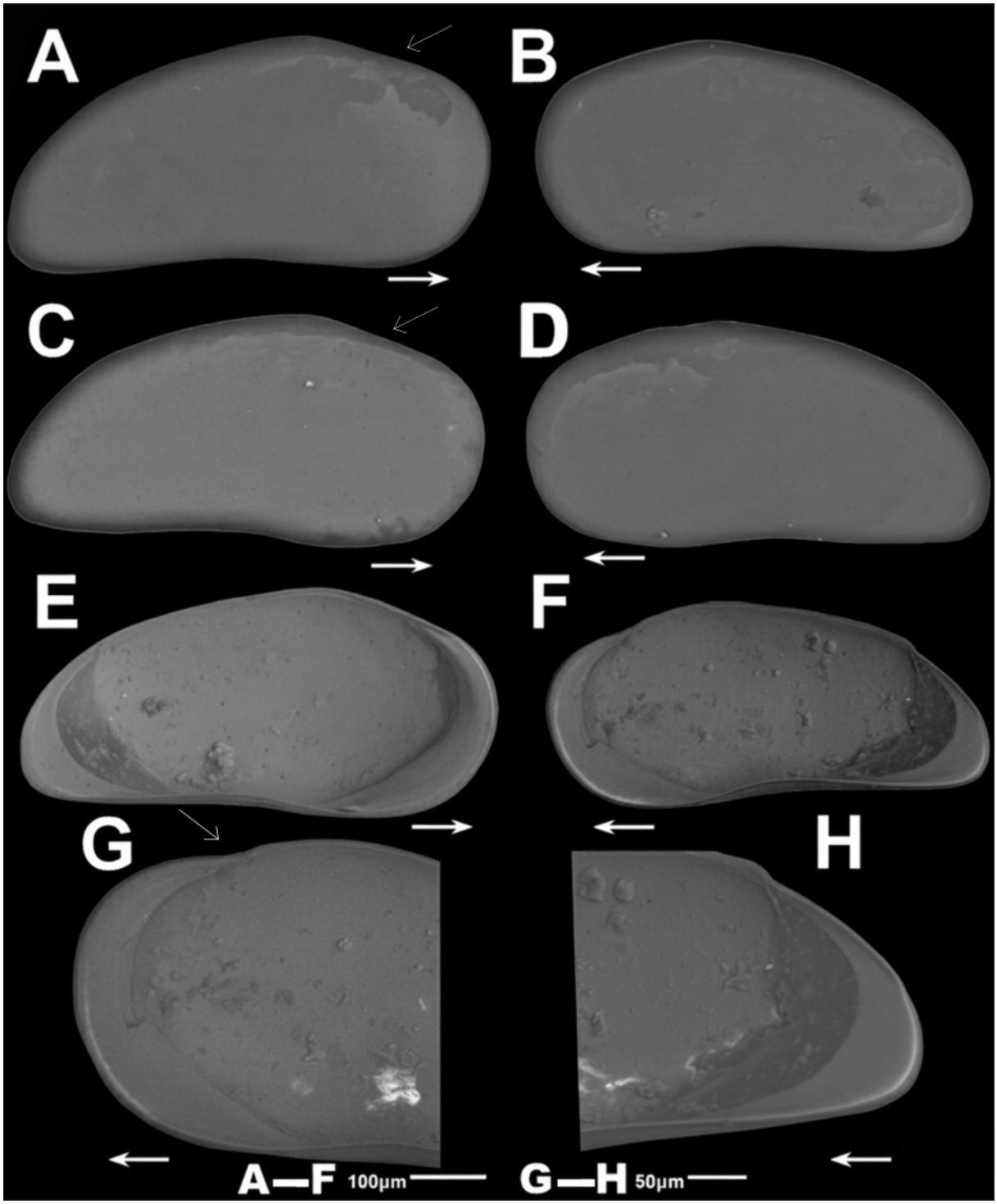


**Fig. 10.** *Thalassocypria zazilha* Macario-González & Cohuo sp. nov., holotype, ♂ (ECO-CH-Z-09320) and allotype, ♀ (ECO-CH-Z-09321). **A, E**. Male right valve, external and internal views, respectively. **B, F**. Male left valve, external and internal views, respectively. **C**. Female right valve external view. **D**. Female left valve external view. **G–H**. Close-ups of male left valve anterior and posterior internal margin, respectively. White thin arrows show antero-dorsal depression in valve morphology. White arrows show the valve orientation toward the anterior margin.

**Male** (holotype)

Carapace. The carapace is compressed (Fig. 10A–B); in lateral view, elongate and subreniform; surface smooth (Fig. 10A–B). LV is slightly larger than RV anteriorly and posteriorly. Dorsal margin arched; sloping steeper towards anterior than posterior end and with a small depression at the first third of the shell. Greatest height is at about one-third of the shell. Anterior margin broadly rounded. Posterior margin acute and narrowly rounded. Ventral margin is slightly concave around the middle. RV (Fig. 10A) is 573.42 µm in length and 265.42 µm in height. Calcified inner lamella equaling 15% anteriorly and 2.6% posteriorly of the total length of shell (Fig. 10E). LV (Fig. 10B) is 586.35 µm in length and 270.33 µm in height. Calcified inner lamella narrow; anteriorly equaling 13.5% and posteriorly 2.56% of total length of shell (Fig. 10F–H). Marginal pore canals are straight. Selvage peripheral. Muscle scars consist of a group of four compact scars centrally located. Hinge adont.

A1 (Fig. 11A). 7-segmented. First segment with one smooth seta antero-medially and with Wouter's organ developed. Postero-distally one long and bare seta that reaches the distal end of the third segment.

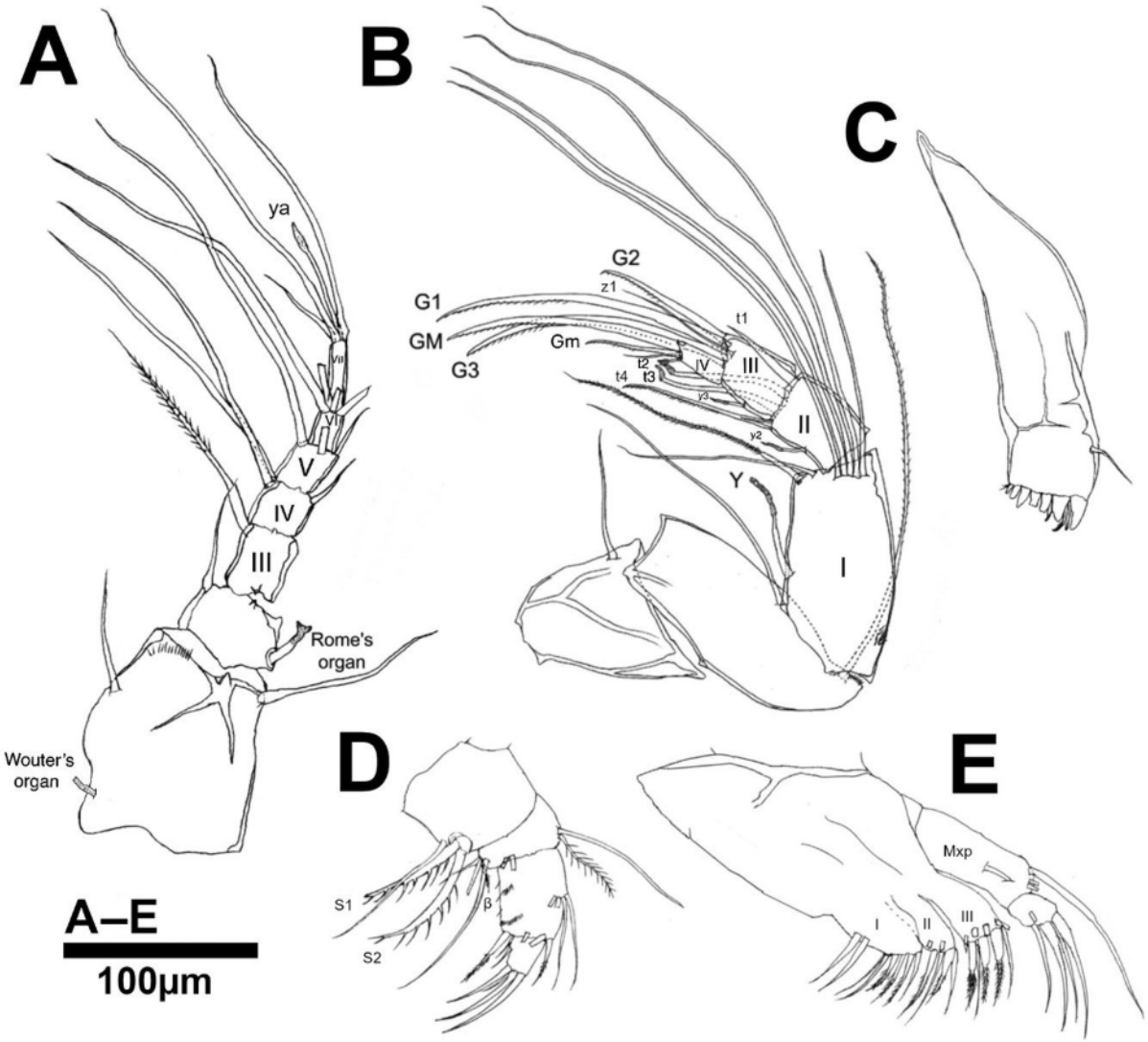


**Fig. 11.** *Thalassocypria zazilha* Macario-González & Cohuo sp. nov., holotype, ♂ (ECO-CH-Z-09320). **A**. A1. **B**. A2. **C**. Md. **D**. Mdp. **E**. Mxl.

Second segment with an apical seta anteriorly. Rome's organ is thick and distally widened. Third segment (III) with one long and serrulate seta. Fourth segment (IV) with two long bare setae anteriorly and one short seta posteriorly. Fifth segment (V) with three setae apically, anterior ones elongated while anterior one is small. Sixth segment (VI) with four setae distally, all of them elongated. Terminal segment with two elongated and one short setae. Aesthetasc (ya) 1.7 times as long as terminal segment. Length ratios of the last 5 segments are as follows: 1.2 : 0.8 : 0.8 : 0.6 : 1.

A2 (Fig. 11B). 6-segmented. Coxa bears one long, bare seta. Basis has one long posterior seta that reaches the distal end of the last segment. Exopod consists of a plate with a single, long, serrulate seta. First endopodal segment (I) with aesthetasc Y, elongated and reaching the distal end of the segment that carries it. Also, postero-distally on this same segment, two unequally long setae; longer one is serrulate. Anteriorly, five natatory setae; four of them exceeding the tips of the claw, while the fifth, which is located more anteriorly, reaches the distal end of the terminal segment. The second endopodal segment (II+II) is divided, with aesthetasc y2 thin and elongated, reaching the distal end of the segment that carries it. Apically on this same segment, t1 and t4 setae claw-like; anterior one (t1) just exceeding the distal end of the following segment, while posterior one (t4) overpassing the distal end of the terminal segment. Male bristles (t2 and t3) are elongated, terminating in rectangular structures. Third endopodal segment (III) with aesthetasc y3 reaching distal segment that carries it. Claws G1 and G3 elongated; 6.6 times as long as terminal segment. Claw G2 short; 3.2 times as long as terminal segment. Only z1 seta was observed. Terminal segment (IV) with GM claw elongated, equaling the length of G1. Claw Gm thin and short; 2.1 times as long as terminal segment. Aesthetasc y4 small.

Md and Mdp (Fig. 11C–D). Coxa with one smooth seta and seven rounded teeth and three additional claw-like. Palp 4-segmented (Fig. 11D). First segment with long and plumose seta S1 and S2. One long seta located most proximally reaches the distal end of the terminal segment. Seta α, not observed. Second segment dorso-distally with two unequally long setae. Four setae ventro-distally of this same segment; two of them long. Seta β is short and plumose. Medially, two additional long setae are present. Third segment dorso-medially with four equally long setae. Apically with five unequally long setae. Terminal segment with four terminal setae; two of them claw-like, and 3.1 times as long as terminal segment.

Mxl and Mxlp (Fig. 11E). Mxl with four endites square-shaped with variable number of setae almost of the same length. First endite (I) with six setae distally and two additional setae located more medially. Second endite (II) square-shaped with six apical setae. Third endite (III) square-shaped with nine apical setae, three of them ("Zahnborsten") serrulate. Palp 2-segmented. First segment with one long seta medially located and three long apical setae. Second segment squarish and distally with two strong claw-like and three smooth setae.

L5 (Fig. 12A–B). Protopodite apically with eleven unequally long setae and a row of four setae slightly more interiorly located. Seta b present. Prehensile palps similar; right one with a finger displaying a steeper middle constriction. Next to the finger are three seta-like structures strongly barbed distally and extending beyond the finger. Left prehensile palp with a curved finger; the three seta-like structures are also present.

L6 (Fig. 12C). 5-segmented. The basal segment bears a setose d1 seta, while d2 is smooth and slightly shorter than d1. Second, third, and fourth segments are all carrying one small apical seta (e, f, g, respectively). The terminal segment is characterized by two distal, thin, and small setae (h1 and h3), as well as a claw (h2). The claw is curved and serrated distally; it is 6.1 times as long as the terminal segment.

L7 (Fig. 12D). 4-segmented. Basal segment with d1, d2, and dp setae. Second segment with a bare and small e-seta apically. Third segment with one short medial f-seta. Terminal segment with very small and

slightly curved h1 and h2 setae. Seta h3 is elongated and serrulate, equaling 5.5 times as long as the terminal segment.

UR AND ATTACHMENT (Fig. 12E). The ramus is robust and slightly hirsute along posterior margin. The anterior Ga-claw is curved and distally serrated, exceeding the middle of the ramus. Anterior Sa-seta small. Posterior Gp-claw curved and distally serrated, just reaching the middle of the ramus. Posterior seta missing, but with two large barbs located at distal third of the ramus. UR attachment is strong and distally bifurcated (Fig. 12E).

HEMIPENIS (Fig. 12F). Small and compact. DL distal end broadly rounded. CL well sclerotized and slightly pointed, not reaching the distal end of the inner lobe. Cp small and ending in a sharp and rounded process. Zenker's organ compressed with six whorls of spines. Internal canals are coiled.

**Female** (allotype)

CARAPACE. Slightly larger than that of males. RV (Fig. 10C) is 645.32 µm in length and 303.74 µm in height. Inner lamella covering 13.23% anteriorly and 3.8% posteriorly of valve length. LV (Fig. 10D) is 680.67 µm in length and 305.42 µm in height. Inner lamella covering 14.2% anteriorly and 4.3% posteriorly of valve length. Valve surface is smooth. LV overlaps RV anteriorly and posteriorly. Hinge adont.

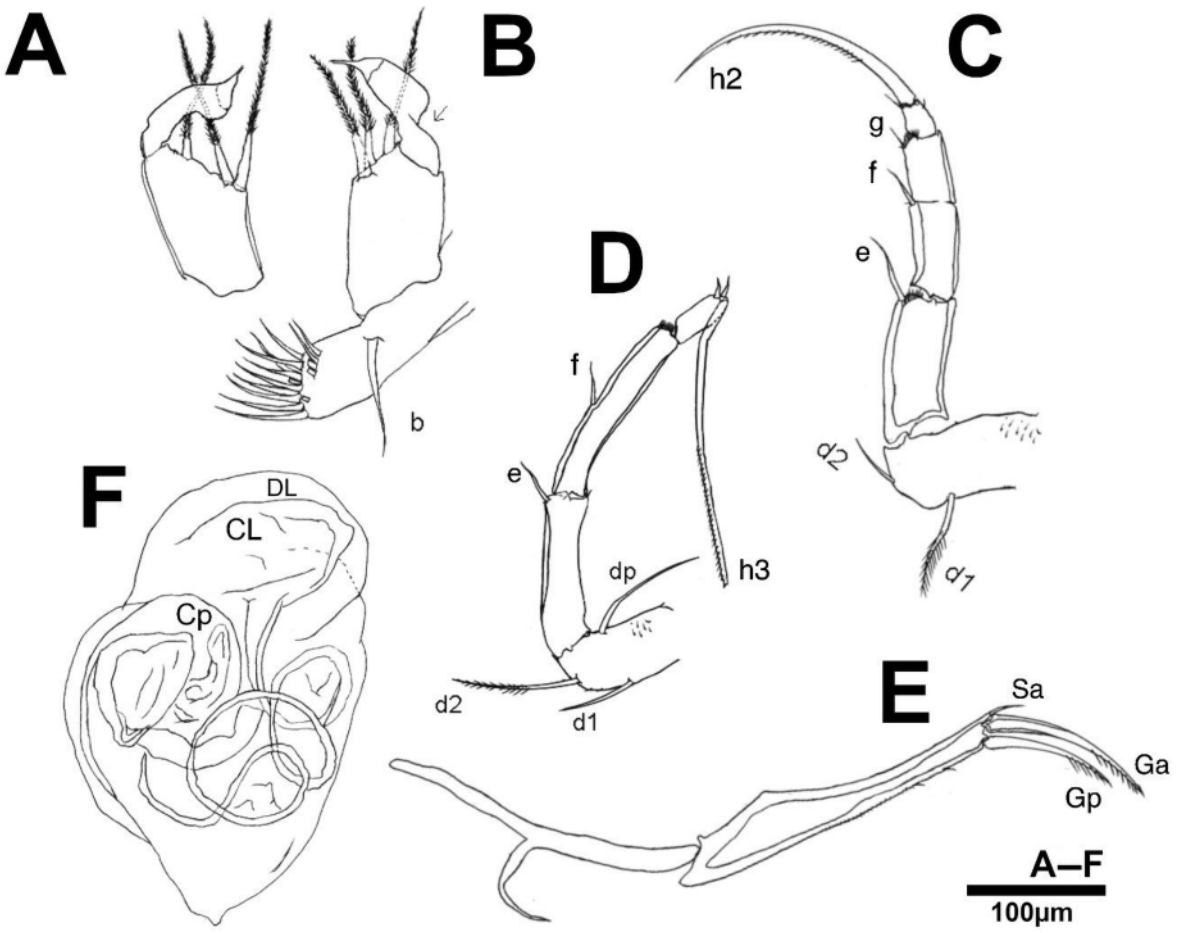


**Fig. 12.** *Thalassocypria zazilha* Macario-González & Cohuo sp. nov., holotype, ♂ (ECO-CH-Z-09320). **A**. Left prehensile palp. **B**. L5 with prehensile palp. **C**. L6. **D**. L7. **E**. UR and attachment. **F**. Hemipenis.

A1 (Fig. 13A). Similar to that of male. First segment anteriorly with Wouter's organ developed and with one long and bare seta distally. Postero-distally on this same segment two long and serrulate setae. Second segment with Rome's organ elongated but not reaching the distal end of the segment. Fourth (IV) and fifth (V) segments with two anterior, long and setose setae and one seta located posteriorly. In the fourth segment (IV), posterior seta is short not exceeding distal end of following segment, whereas in fifth segment (V) it is long, almost exceeding the distal end of terminal segment. Sixth segment (VI) with five apical setae. Aesthetasc ya elongated, 3.1 times as long as terminal segment.

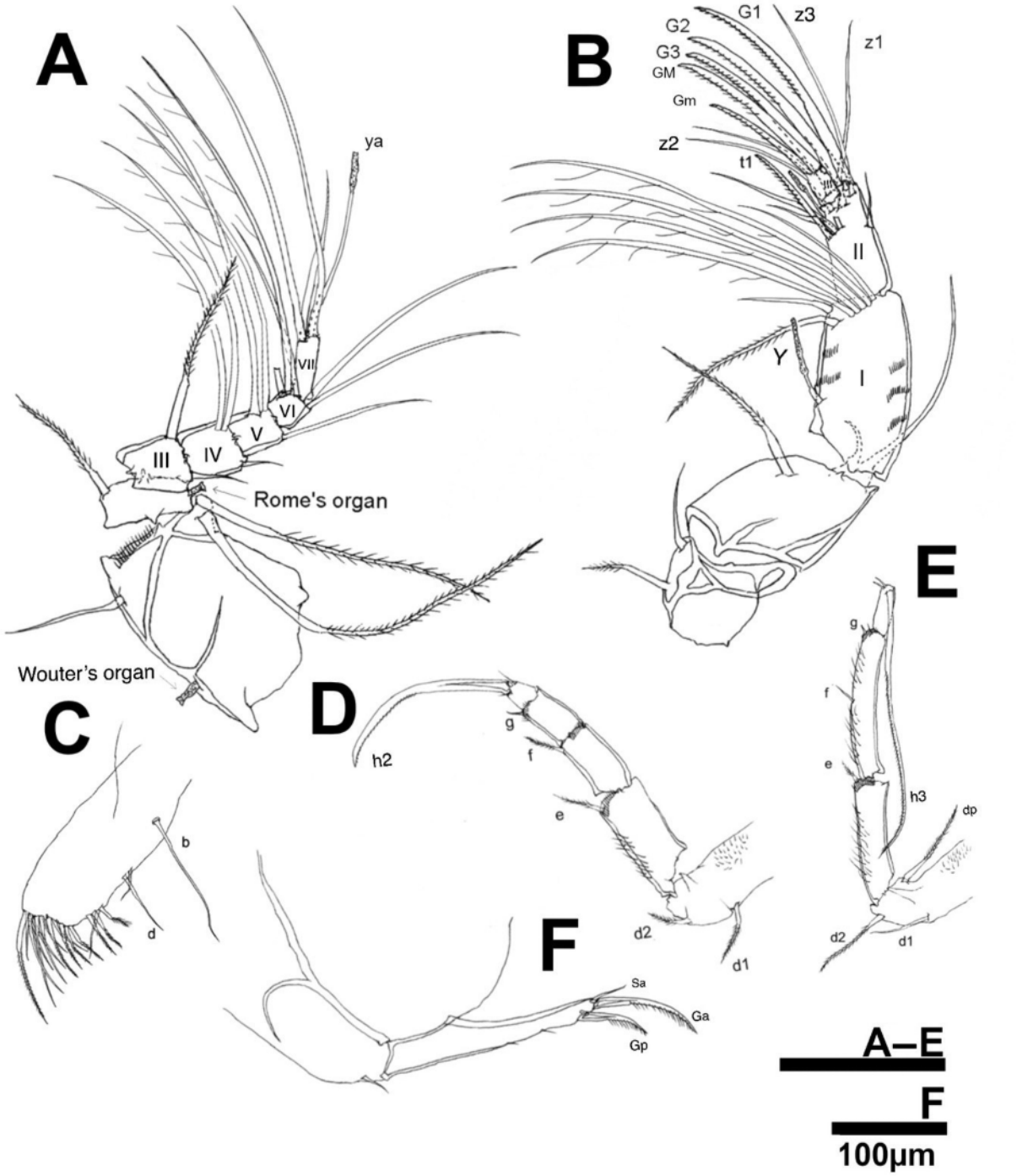


**Fig. 13.** *Thalassocypria zazilha* Macario-González & Cohuo sp. nov., allotype, ♀ (ECO-CH-Z-09321). **A**. A1. **B**. A2. **C**. L5. **D**. L6. **E**. L7. **F** UR and the sexual field.

A2 (Fig. 13B). 5-segmented and sexually dimorphic. Coxa with two setae posteriorly. Exopod consists of a plate and two setae; the longer one exceeding the distal end of the following segment. Natatory setae are slightly setulae. All "t" setae present; t1 is claw-like and distally serrulate. The three "z" setae are elongated, not reaching the tip of the claws. Claws G1, G2, and G3 are subequally long and 6.8 times as long as terminal segment. Claw GM equally long than G1, while Gm shorter reaching 3.7 times the length that carries it.

Md, Mdp and Mxlp. Similar as in males.

L5 (Fig. 13C). Carries seventeen smooth or serrulate setae on protopodite. Setae b and d present. A small seta attached next to td seta is present.

L6 (Fig. 13D) and L7 (Fig. 13E). Hirsute with all setae serrulate, similar as in males.

Genital field (Fig. 13F). Broadly rounded; no projections observed. One small and smooth seta is located below the UR.

**Differential diagnosis**

The genus *Thalassocypria* currently comprises 6 nominal species (*T. aestuarina* Hartmann, 1957, *T. elongata* Hartmann, 1957, *T. gesinae* Keyser, 1975, *T. lacuscola* Hartmann, 1980, *T. sarbui* Maddocks & Iliffe, 1993, and *T. vavrai* Keyser, 1975), all related to marine or estuarine environments. *Thalassocypria zazilha* sp. nov. is, therefore, the only species recorded to date in a freshwater environment. Morphologically, this species is more closely related to the Central American *T. aestuarina* and *T. elongata*. The shell morphology between these three species is very similar, with a small depression anterodorsally and with slightly more elongated valves compared with the new species. Male sexual appendages differentiate the species: *T. aestuarina* has the outer and middle lobes distally pointed, and *T. elongata* has the outer lobe largely elongated. In contrast, *T. zazilha* has the lobes broadly rounded. This species also has the left prehensile palp with a small contraction in the middle of the finger, which is absent in all other species.

**Remarks**

This species was found in the water column and among submerged vegetation, suggesting swimming capabilities, particularly in juvenile stages. The known distribution of this species is apparently restricted to a few lakes (Bacalar, Milagros, and Estero Chac) within the hydrological system; nonetheless, its distribution within the estuarine environments of Chetumal Bay remains uncertain. Therefore, at this point, this species is considered a possible endemic to the Bacalar hydrological system. Average environmental conditions of sampling sites where this species was found: temperature 30.5°C, dissolved oxygen 7.4 mg $l^{-1}$, pH 8.31, and conductivity 2120 µS $cm^{-1}$.

Genus *Dolerocypria* Tressler, 1937

***Dolerocypria maanik*** Macario-González & Cohuo sp. nov.
urn:lsid:zoobank.org:act:1DE6CDF1-5A88-4E31-AEED-B6284F07BF00
Figs 14–17

**Diagnosis**

Relatively small individuals (< 650 µm) with elongated and trapezoidal-shaped valves. Greatest height in first third of the valve. LV slightly overlaps RV anteriorly and posteriorly. Female slightly larger than male. On A2, natatory setae do not reach the tips of the terminal claws. Mxlp second segment with five setae, of which two are claw-like. Male prehensile palps are almost symmetrical, fingerhook-shaped at about 90°. Hemipenis with distal shield triangular in shape and a squarish body. Female sexual fields with two prominent digitiform projections.

**Etymology**

The epithet "*maanik*" was proposed by Juan Manuel Salazar Montes, a biology student from the Instituto Tecnólogico de Chetumal, as part of a local contest to name the species. In the Mayan language, this word means "highly important" and alludes to the relative ecological role of this species in the environments where it is found, and the relevance of its adaptation from marine to freshwaters. The name should be treated as a noun in apposition.

**Type material**

**Holotype**

MEXICO • ♂; Quintana Roo State, Lake Milagros; 18°51′5065″ N, 88°41′6635″ W; 6 m a.s.l.; 20 Aug. 2024; ECO-CH-Z-12547.

**Allotype**

MEXICO • ♀; Quintana Roo State, Lake Milagros; 18°51′5065″ N, 88°41′6635″ W; 6 m a.s.l.; 20 Aug. 2024; ECO-CH-Z-12550.

**Paratypes**

MEXICO • 1 ♂; Quintana Roo State, Lake Milagros, 18°51′5065″ N, 88°41′6635″ W; 6 m a.s.l.; 20 Aug. 2024; preserved on one slide and in a paleontological slide; ECO-CH-Z-12549, ECO-CH-Z-12556 • 1 ♀; same collection data as for preceding; preserved on one slide and in a paleontological slide; ECO-CH-Z-122548, ECO-CH-Z-12556.

**Localities**

Littoral sediments of Lake Milagros, Quintana Roo Federal State, Mexico. Other sites where this species has been observed, Lake Bacalar.

**Description**

Measurements. Males: the RV (Fig. 14A, E) measures 630±95 μm in average length and 202.9±88 μm in average height (n=2). The LV (Fig. 14B, F) measures 637.2±92 μm in average length and 203±90 μm average height (n=2). Females: the RV is 635.3±87 μm in average length and 209.2±75 μm in average height (n=2). The LV (Fig. 14D) measures 640.5±92 μm in average length and 208.1±81 μm in average height (n=2).

**Male** (holotype)

Carapace. Elongated in lateral view (Fig. 14A–B). LV is slightly larger than RV both anteriorly and posteriorly. The dorsal margin with greatest height in the anterior third of the shell, then gently sloping toward the posterior end (Fig. 14A–B). The anterior margin is rounded and bears a few marginal pore canals. The posterior margin is narrow and rounded, with a few marginal pore canals. The ventral margin is concave at mid-length. The RV (Fig. 14A, E) measures 688.2 μm in length and 235 μm in height. The calcified inner lamella is relatively wide, comprising approximately 22% of the total shell length anteriorly and 27% posteriorly (Fig. 14G–H). The LV (Fig. 14B, F) measures 688.2 μm in length and 233 μm in height. Calcified inner lamella similar to that of the RV (Fig. 14F). Muscle scars consist of four compacted scars and two more anteriorly positioned mandibular scars. Shell surface smooth, sparsely covered with short setae. Hinge adont.

A1 (Fig. 15A). 7-segmented. First segment carries two long setae posteriorly and one short seta anteriorly. Second segment with Rome's organ strongly developed, anteriorly with a short seta, reaching the middle of the next segment. Third segment (III) with two setae distally located, the anterior one reaching the end of the fifth segment. Fourth (IV) and fifth (V) segments both have one short seta posteriorly and two long setae anteriorly, about 11 times as long as the last segment. Sixth segment (VI) with four setae distally located. The one located more posteriorly is shorter, about 7 times as long as the last segment. Seventh segment (VII) with three setae and an aesthetasc about five times as long as the segment that carries it. Length ratio of endopodal segments: 1:1.4:1:1.8:1.4.

A2 (Fig. 15B, B'). 6-segmented. First segment with two posteriorly positioned setae. Second segment with a long posterior seta that exceeds the length of the following segment. Exopod is represented by two setae, the longer one does not reach the end of the next segment. First endopodal segment (I) has a long Y-aesthetasc posteriorly and a long distal seta. Natatory setae are represented by four long setae, each approximately 11 times as long as the last segment, and an additional shorter seta, about five times as long as the last segment. Second endopodal segment (II) bears four distally located setae, two of

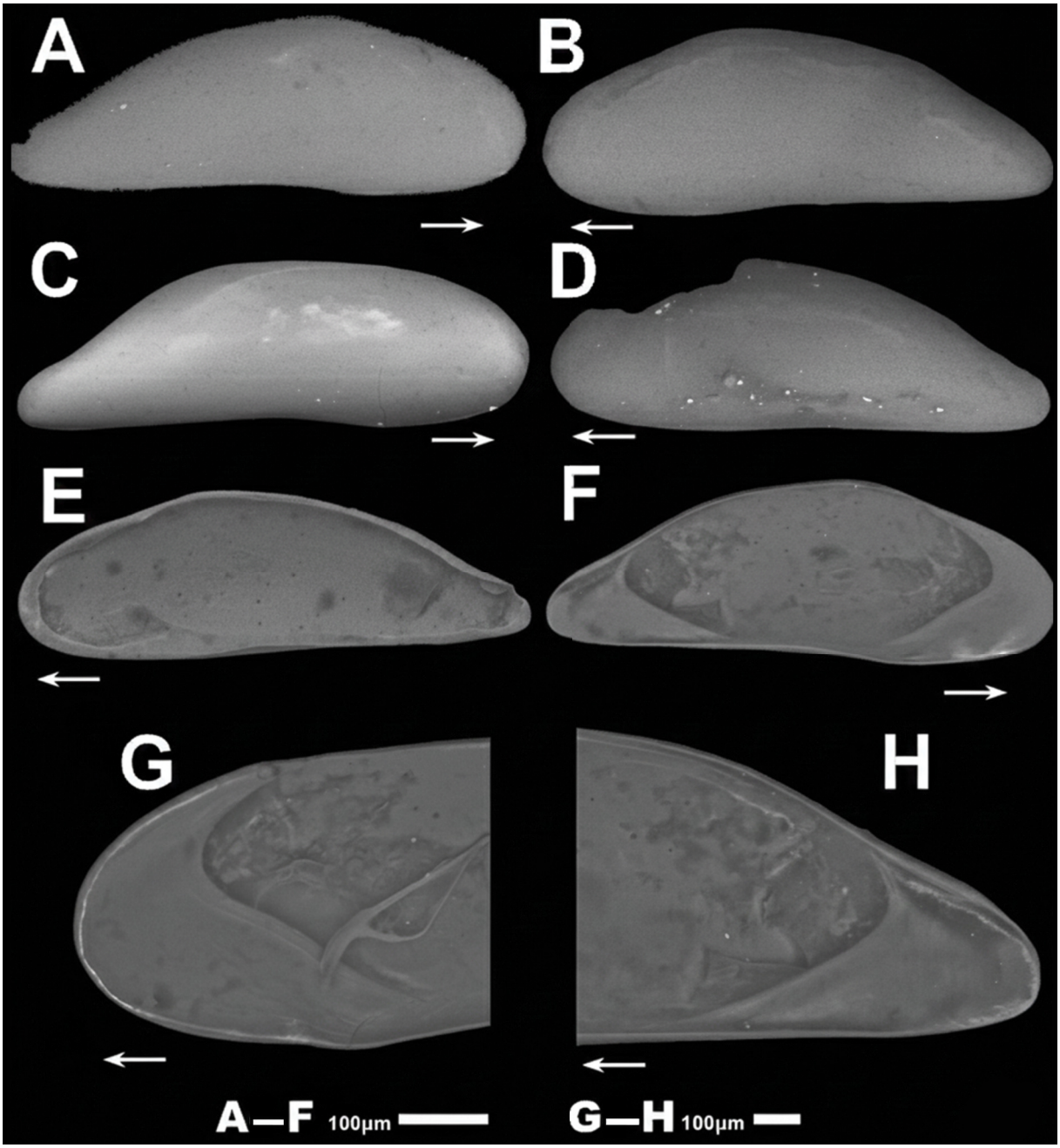


**Fig. 14.** *Dolerocypria maanik* Macario-González & Cohuo sp. nov., holotype ♂ (ECO-CH-Z-12547) and allotype, ♀ (ECO-CH-Z-12550). **A, E**. Male right valve, internal and external views, respectively. **B, F**. Male left valve, internal and external views, respectively. **C**. Female right valve, external view. **D**. Female left valve, external view. **G–H**. Close-ups of male anterior and posterior margin, internal view. White arrows show the valve orientation toward the anterior margin.

which are transformed into male sexual bristles (t2, t3), both of which extend beyond the distal segment. Posterior-most seta (t1) is claw-like. Third endopodal segment (III) has a small aesthetasc (y2) located medially. G2 claw is reduced, measuring approximately 3.5 times as long as the final segment. G1 and G3 claws are well developed, each about 10 times as long as last segment. Fourth endopodal segment (Fig. 15B') carries a long GM claw, with the same length of G1 and G3. Gm claw, reduced about 2.5 times as long as the segment.

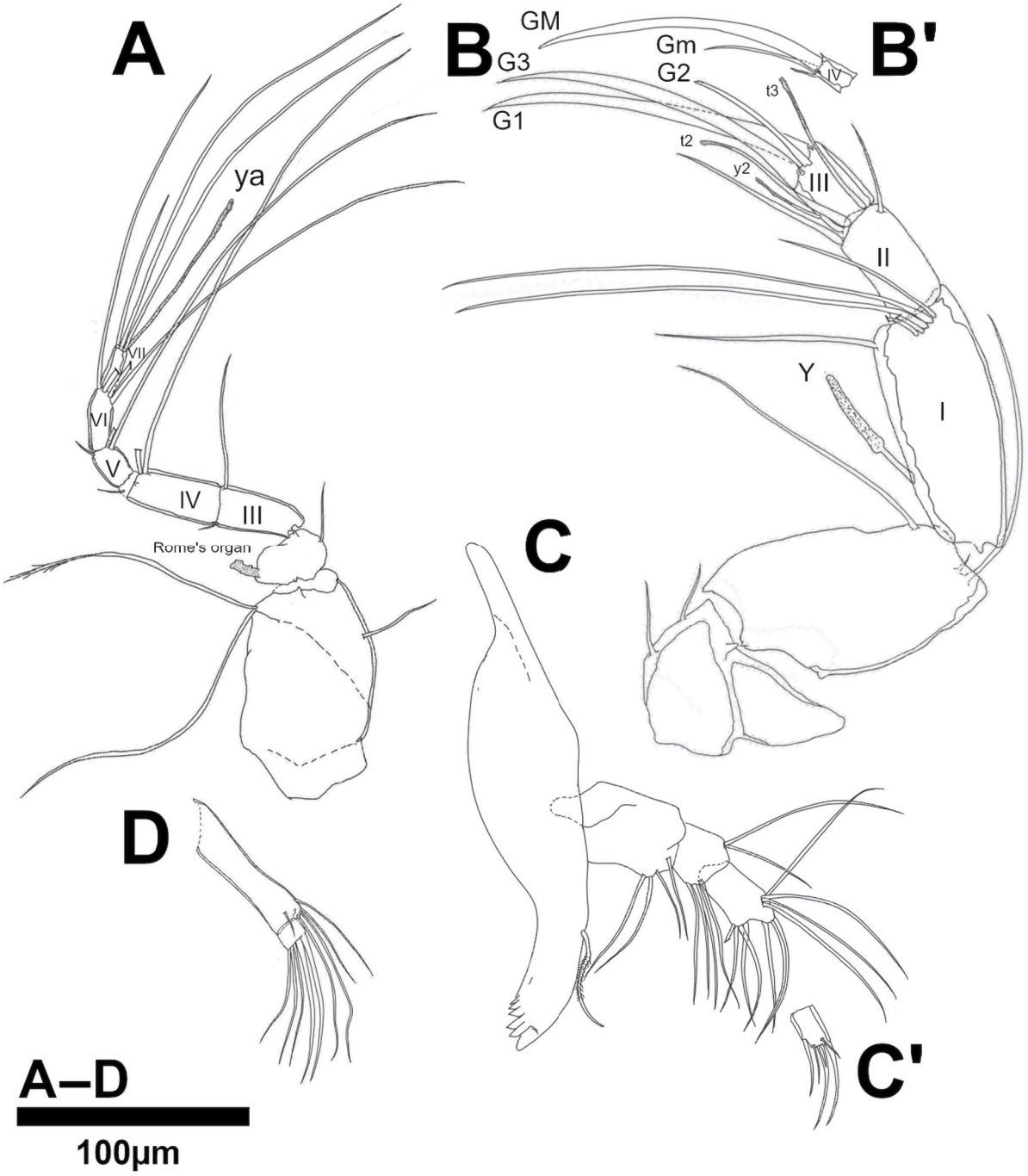


**Fig. 15.** *Dolerocypria maanik* Macario-González & Cohuo sp. nov., holotype ♂ (ECO-CH-Z-12547). **A**. A1. **B, B'**. A2. **C, C'**. Md and Mdp. **D**. Mxlp.

Md and Mdp (Fig. 15C, C'). Coxa is represented by a masticatory plate bearing approximately 10 teeth and one long serrulate seta. Palp is 4-segmented. First segment has four bare setae ventrally. Second segment bears four ventral setae of equal length and two dorsal setae of unequal length. Third segment with eleven distally located setae, all of approximately equal length. Fourth segment (Fig. 15C') with three claw-like setae, each about 1.5 as long as the segment itself, along with two short setae.

Mxlp (Fig. 15D). 2-segmented, first segment bears five setae. Second segment is square-shaped and with five setae, two of which are claw-like.

L5 (Fig. 16A–B). Protopodite with nine distal setae. Setae a, b and d present. Prehensile palps are similar, hook-like at an angle of almost 90°. Each palp has two long, robust basal setae. Left palp a slightly more developed finger than the right one.

L6 (Fig. 16C). 5-segmented. First segment bears setae d1 and d2. Second, third, and fourth segments each bear a very short e, f, and g seta, respectively. Fifth segment is square-shaped and carries a long claw h2, 8.3 times as long as terminal segment.

L7 (Fig. 16D). 4-segmented. First segment with setae d1, d2, and dp. Second segment has a distal e-seta that does not reach the midpoint of the next segment. Third and fourth segments are fused, bearing two setae, f-seta located medially and g-seta distally. Fourth segment with two very short setae (h1 and h2), and a long, robust and hirsute h3 seta that exceeds the combined lengths of the preceding three distal segments.

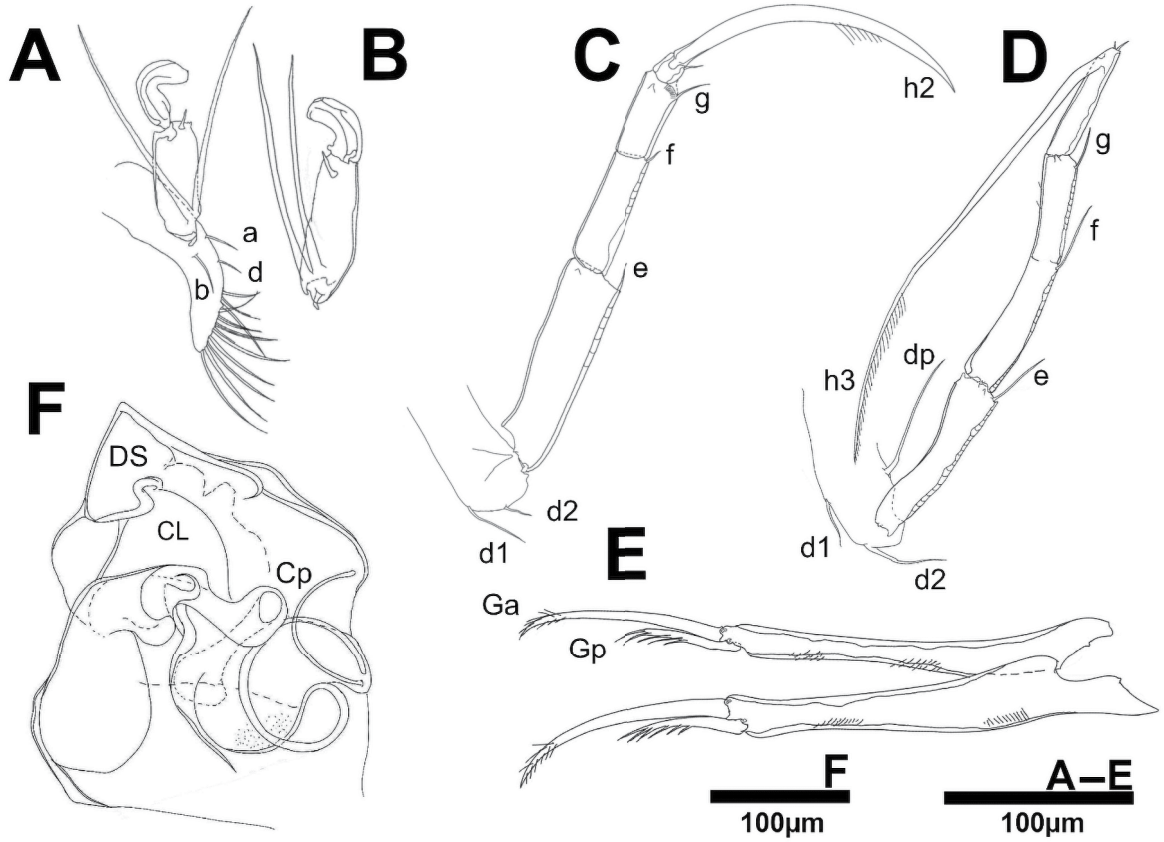


**Fig. 16.** *Dolerocypria maanik* Macario-González & Cohuo sp. nov., holotype ♂ (ECO-CH-Z-12547). **A**. L5 with left prehensile palps. **B**. Right palp. **C**. L6. **D**. L7. **E**. UR. **F**. Hemipenis.

UR (Fig. 16E). Ramus is robust and hirsute. Ga claw is strong and long, exceeding half the length of the ramus. Gp claw is shorter, with well-developed spines, and reaching only about half the length of the anterior claw. No anterior or posterior setae are observed.

Hemipenis (Fig. 16F). DS is triangular, the body is square-shaped. CL triangular shaped. The Cp is curved and exhibits a clasping appearance. Zenker's organ compressed with 7 whorl of spines.

**Female** (allotype)

Carapace. Elongated, similar in shape and size to that of the male, but slightly larger. Surface of valves is smooth and covered by few hairs. LV is larger than RV both anteriorly and posteriorly. The RV is 690.14 µm in length and 260 µm in height, with greatest height located in the anterior third (Fig. 14C). Inner lamella covers 23.4% of the total length anteriorly and 20.6% posteriorly. LV (Fig. 14D) measures 705 µm in length and 263.5 µm in height, also with the greatest height in the anterior third. Inner lamella covers 24.4% anteriorly and 20% posteriorly. Hinge adont.

A1 (Fig. 17A). 7-segmented. First five segments are as in the male. The sixth segment (VI) bears three setae, with the anterior ones elongated, measuring 11.3 times as long as the terminal segment. Seventh segment (VII) carries two elongated setae, one short seta, and one aesthetasc (ya), which is 1.5 times as long as the segment.

A2 (Fig. 17B). 5-segmented, sexually dimorphic. Coxa and basis are similar to those of the male. First endopodal segment (I) bears two unequally long posterior setae. Natatory setae are represented by four long and one short seta, none of which reach the terminal claws. Second endopodal segment (II) shows three t-setae, with t1 being claw-like. Three z-setae are present, relatively short and slightly exceeding half the length of the terminal claws.

G1, G2, and G3 claws. Similar to those in the male, G3 short. Terminal segment with a well-developed GM claw, while the Gm is reduced to a seta.

Md, Mdp, Mxl, and Mxlp. As in males.

L5 protopodite. Distally with 8–10 distal setae, setae a, b, and d are present.

L6 (Fig. 17C). Basal segment with setae d1 and d2, shorter than in the male. The second, third, and fourth segments bear very short setae e, f, and g, respectively. Last segment carries a strong, long h2 claw that exceeds the combined length of the three preceding segments.

L7(Fig. 17D). Similar to male.

UR and sexual field (Fig. 17E). The UR is similar to that of the male, with the attachment being distally bifurcated. Sexual field is represented by two digitiform projections, attached to the posterior part of the body. Such projections are accommodated in the elongated posterior part of the carapace.

**Differential diagnosis**

Species of the genus *Dolerocypria* are commonly found in marginal marine and brackish waters, such as bays, (totally dark) caves, anchialine, and in temporary freshwater environments like rock pools in the foreshore, across a broad range of salinities (Maddocks & Iliffe 1993). Currently, approximately 12 species are recognized, most of them marine, although eight are also distributed in coastal areas: *Dolerocypria convoluta* Maddocks, 1993, *Dolerocypria elongata* (Hartmann, 1955), *Dolerocypria ensigera* Maddocks, 1992, *Dolerocypria fastigata* Keyser, 1976, *Dolerocypria heylenae* Wouters, 2001, *Dolerocypria iliffei* Maddocks, 2005, *Dolerocypria mukaishimensis* Okubo, 1980, and *Dolerocypria*

*taalensis* Tressler, 1937. Despite their wide global distribution, most species show a similar valve morphology, and the majority are currently known from the Pacific island region (Meisch *et al*. 2024). *Dolerocypria maanik* sp. nov. is closely related to *D. convulata* from Jamaica (Maddocks & Iliffe 1993) and *D. fastigata* from southern Florida (Keyser 1975). *Dolerocypria convoluta* displays a similar valve shape, but it has a relatively smaller (560 µm length and 200 µm height) than *D. maanik* (630 µm length and 208 µm height). Sexual appendages also differ: in *D. convoluta*, the prehensile palps are wedge-shaped, and one of them is curved in a sigmoid fashion, the other hook-like with a squarish finger forming a 90° angle; in *D. maanik*, both palps are hook-like with more rounded fingers. The hemipenis

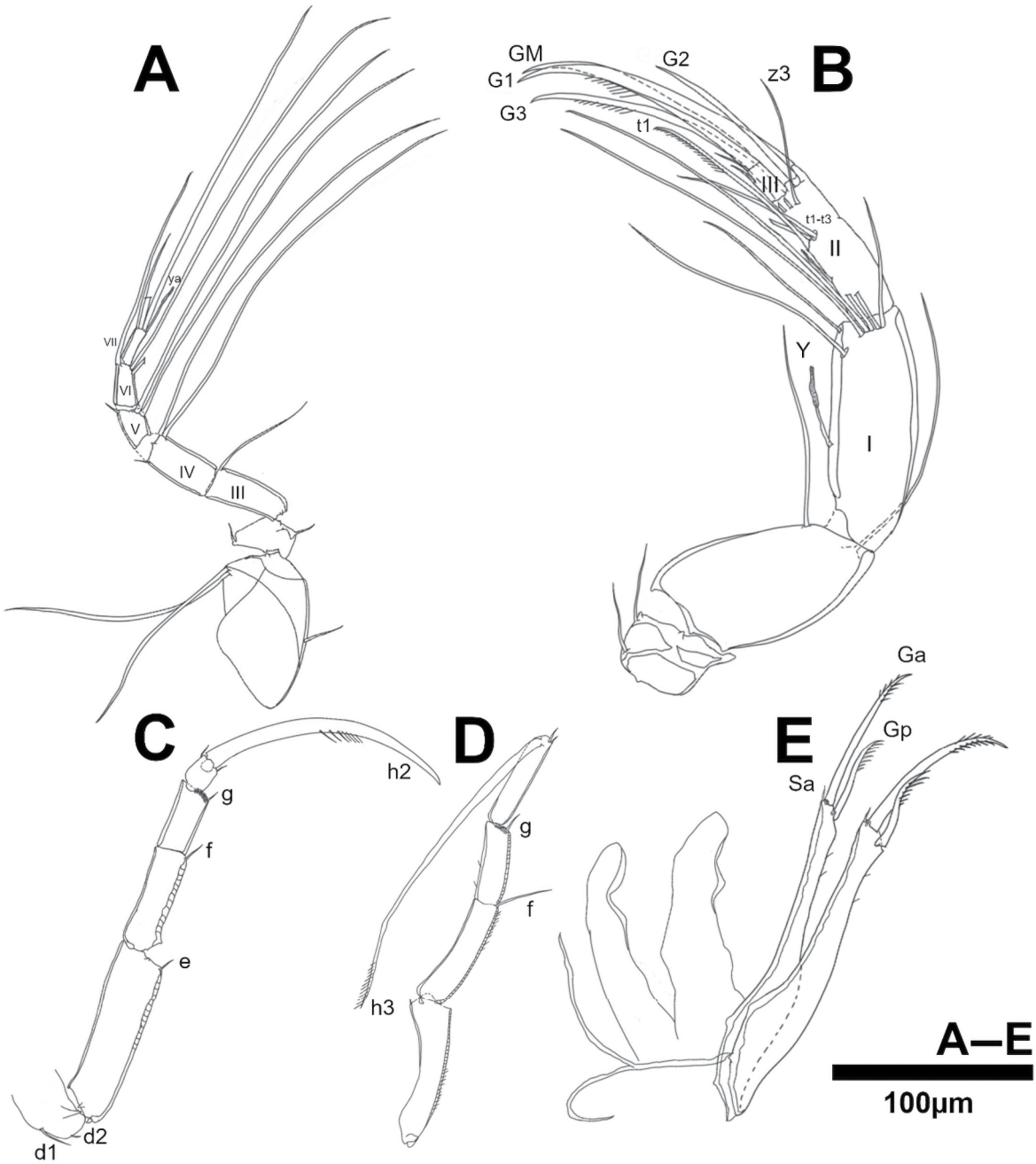


**Fig. 17.** *Dolerocypria maanik* Macario-González & Cohuo sp. nov., allotype, ♀ (ECO-CH-Z-12550). **A**. A1. **B**. A2. **C**. L6. **D**. L7. **E**. UR, attachment, and sexual field.

is also distinguishable between species. In *D. convoluta*, the distal shield is square-shaped, whereas in *D. maanik*, it is triangular. *Dolerocypria fastigata* has a similar valve size to *D. maanik* but the outline differs: valves in *D. fastigata* are more compressed, particularly in the middle to posterior region. The calcified inner lamella is much broader in *D. maanik*, while in *D. fastigata*, it does not exceed 10% anteriorly and 15% posteriorly. The prehensile palps in *D. fastigata* are short and stout, with one finger positioned at an obtuse angle (~135°). In *D. maanik*, the palps are more elongated, and both fingers are positioned at approximately 90°. The hemipenis in both species has a triangular distal shape, but in *D. fastigata*, the copulatory process (Cp) appears pointed and even exceeds the length of the distal shield, whereas in the new species it is hook-like. The anterior seta on the uropod is present in *D. fastigata* but absent in *D. maanik*.

**Remarks**

The average environmental variables at the sampling site were: temperature 32.5°C, dissolved oxygen 7.53 mg $l^{-1}$, and conductivity 2970 µS $cm^{-1}$.

Family Cytherideidae Sars, 1925
Subfamily Cytherideinae Sars, 1925
Genus *Cyprideis* Jones, 1857

***Cyprideis ichkabal*** Macario-González & Cohuo sp. nov.
urn:lsid:zoobank.org:act:58E5D66F-519A-4276-AD3F-9CBFBDC95EBC
Figs 18–22

**Diagnosis**

Relatively large ostracodes (> 900 µm), with sexually dimorphic shells: males are larger than females, and females bear distinct nodes on the valve surface, which are absent in males. Valves are compressed and relatively rectangular. LV is larger than RV both anteriorly and posteriorly. Exopod of A2 is represented by a long and slender seta that exceeds the distal end of the terminal segment. The distal shield of the hemipenis is triangular and sharply pointed. The female sexual field is triangular, ending in a broad triangular process.

**Etymology**

Ichkabal is an ancient Mayan city located near Lake Bacalar, and it means “place within lowlands”. This name was chosen because the species inhabits wetlands in the Bacalar system. The name was proposed by Rosaura Castro Camara as part of a local contest to name the species. It should be treated as a noun in apposition.

**Type material**

**Holotype**

MEXICO • ♂; Quintana Roo State, Lake Bacalar; 18°64′5267″ N, 88°40′8571″ W; 0.4 m a.s.l.; 20 Aug. 2024; soft parts dissected in one slide (ECO-CH-Z-12542), and valves preserved in paleontological slide (ECO-CH-Z-12553); ECO-CH-Z-12542, ECO-CH-Z-12553.

**Paratype**

MEXICO • 1 ♀; Quintana Roo State, Lake Bacalar, 18°64′5267″ N, 88°40′8571″ W; 0.4 m a.s.l.; 20 Aug. 2024; soft parts dissected in one slide (ECO-CH-Z-12543), and valves preserved in paleontological slide (ECO-CH-Z-12553); ECO-CH-Z-12543, ECO-CH-Z-12553.

**Other material**

MEXICO • 3 ♀♀, 3 ♂♂ carapaces; same collection data as for holotype; ECO-CH-Z-12557.

**Localities**

Sediments of Lake Bacalar, Quintana Roo federal state. Mexico. Other sites where the species has been observed are Laguna Guerrero and Laguna Chile Verde.

**Description**

Measurements. Males: the RV (Fig. 18A) measures 920.5±110 μm in average length, and 483.7±95 μm in average height (n=4). The LV (Figs 18B, 19A, E–F) measures 940.1±98 μm in average length and 487.6±87 μm in average height (n=4). Females: the RV (Fig. 18C) is 836.2±64 μm in length and 458±57 μm in height (n=4) at the first third of the valve (greatest height). LV (Fig. 18D) measures 866.5±72 μm in average length and 507.1±53 μm in average height (n=4) at the same position.

**Male** (holotype)

Carapace. In lateral view, it is relatively square-shaped (Fig. 18A–B). LV is larger than RV both anteriorly and posteriorly. Dorsal margin is gently arched, with the greatest height located in the anterior first third of the shell. Anterior and posterior margins are rounded and slightly downward-projected. Ventral margin is nearly straight, slightly concave in the mouth region. Right valve (Fig. 18A) measures 1010.3 μm in length, and 495.8 μm in height, with maximum height at the anterior third. Calcified inner lamella is relatively narrow, covering less than 10% anteriorly and 5.6% posteriorly. The LV (Figs 18B, 19A, E–F) measures 1042.1 μm in length and 501.4 μm in height, with the greatest height in the anterior third. Its calcified inner lamella is narrow (Fig. 19E–F). and similar to that of the RV. Marginal pore canals are straight, with more than 40 present both anteriorly and posteriorly. Muscle scars consist of four compact (Fig. 19F), aligned scars and two additional mandibular scars located more anteriorly. Hinge (Fig. 19B) elongated in left valve with three elements, posterior element with few toothlets (<5), medial element with about 17 very small sockets, anterior element (Fig. 19B) with about 15 teeth. Right valve hinge complementary, with comparable number of teeth, toothlets and sockets. The shell surface is pitted and sparsely covered by short hairs. Nodes (tubercles) are absent in males.

A1 (Fig. 20A). 5-segmented. First segment is hirsute, without a seta observed. Second segment bears a strong posterodistal seta that exceeds the end of the terminal segment. Third segment (III) has a strong, short seta that reaches the middle of the terminal segment. Fourth segment (IV) has three unequally long setae anteromedially, and one short seta that does not reach the end of the segment. Distally, this same segment bears one thin seta and one strong claw-like seta. Terminal segment (V) carries two claw-like setae and one aesthetasc.

A2 (Fig. 20B). 5-segmented. First and second segments are hirsute and lack setae. Exopod represented by a spinneret seta remarkable slender, with two constrictions at the ends of first and second third extending beyond the terminal segment. First endopodal segment (I) segment bears bunches of long hairs and a posterodistal seta not reaching the end of the next segment. Second endopodal segment (II) carries three posteromedial setae, one posterodistal claw-like seta, and two anteromedial setae of unequal length. Third endopodal segment (III) with two strong claws, each 4.3 times as long as the segment that carries them.

Md and Mdp (Fig. 20C). Coxa consists of a masticatory plate with a row of 11 teeth and one short seta widened at the base. Palp is four-segmented. First segment bears a single long, hirsute ventral seta. Second segment has four unequally long distal setae, the longest of which exceeds the terminal segment. Third segment with four unequally long posterodistal setae and three anterodistal setae. Fourth segment with three claw-like setae, each 3.8 times as long as the segment, and one short claw-like seta.

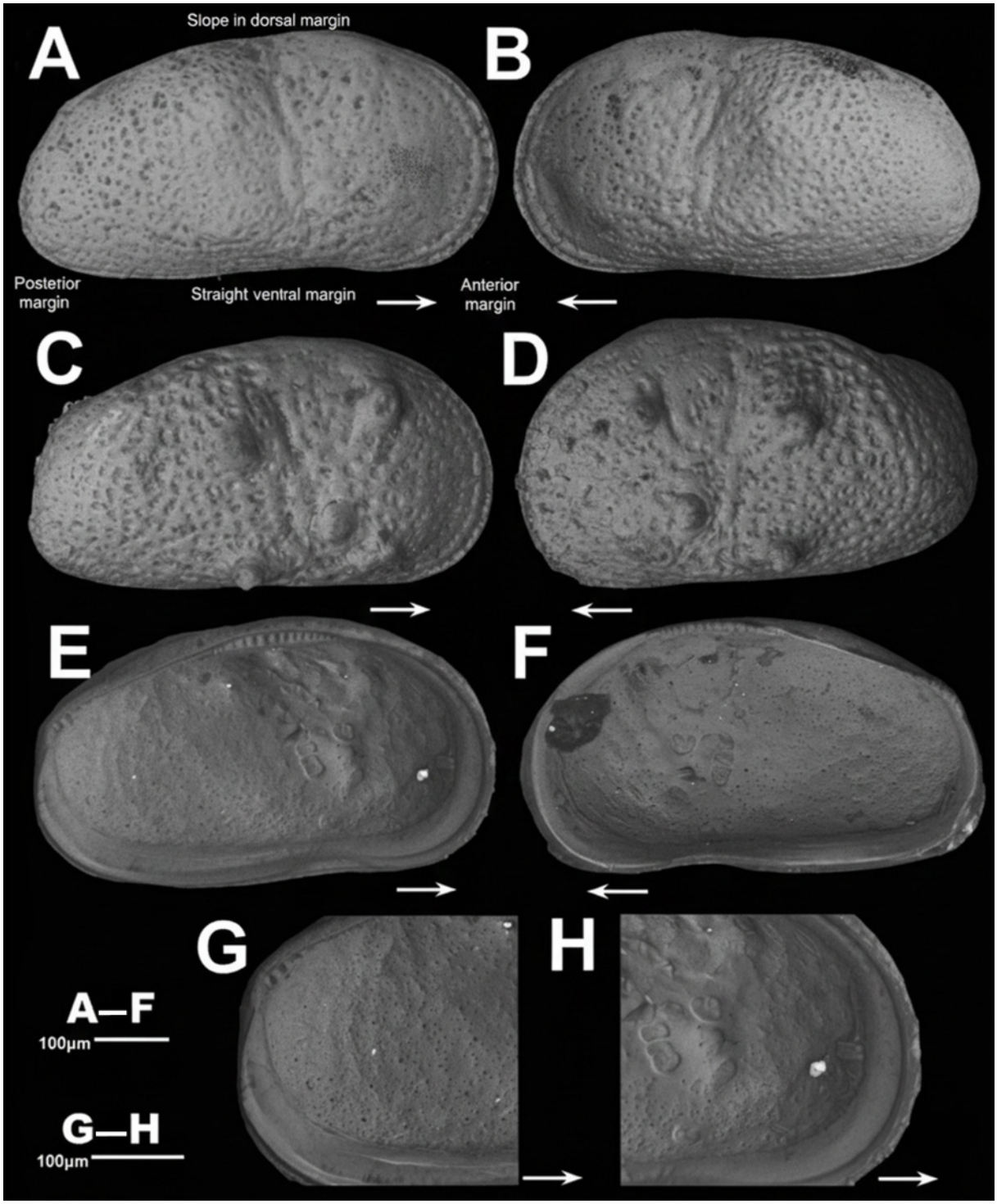


**Fig. 18.** *Cyprideis ichkabal* Macario-González & Cohuo sp. nov., holotype, ♂ (ECO-CH-Z-12542, ECO-CH-Z-12553) and paratype, ♀ (ECO-CH-Z-12553). **A**. Male right valve, external view. **B**. Male left valve, external view. **C, F**. Female right valve, external and internal views, respectively. **D–E**. Female left valve, external and internal views, respectively. **G–H**. Close-up of female valve posterior and anterior margins, respectively. White arrows show the valve orientation toward the anterior margin.

MXLP (Fig. 20D). 2-segmented. First segment with four setae, hirsute, and has one claw-like seta. Second segment with three claw-like setae.

BRUSH-LIKE ORGANS (Fig. 20E). Elongated with a group of 11–5 long apical setae.

L5 (Fig. 21A). Protopodite with four strong, hairy setae. Second segment with one strong distal seta. Third segment lacks a distinct seta. Fourth segment has one strong claw and a thin seta that just exceeds the base of the claw.

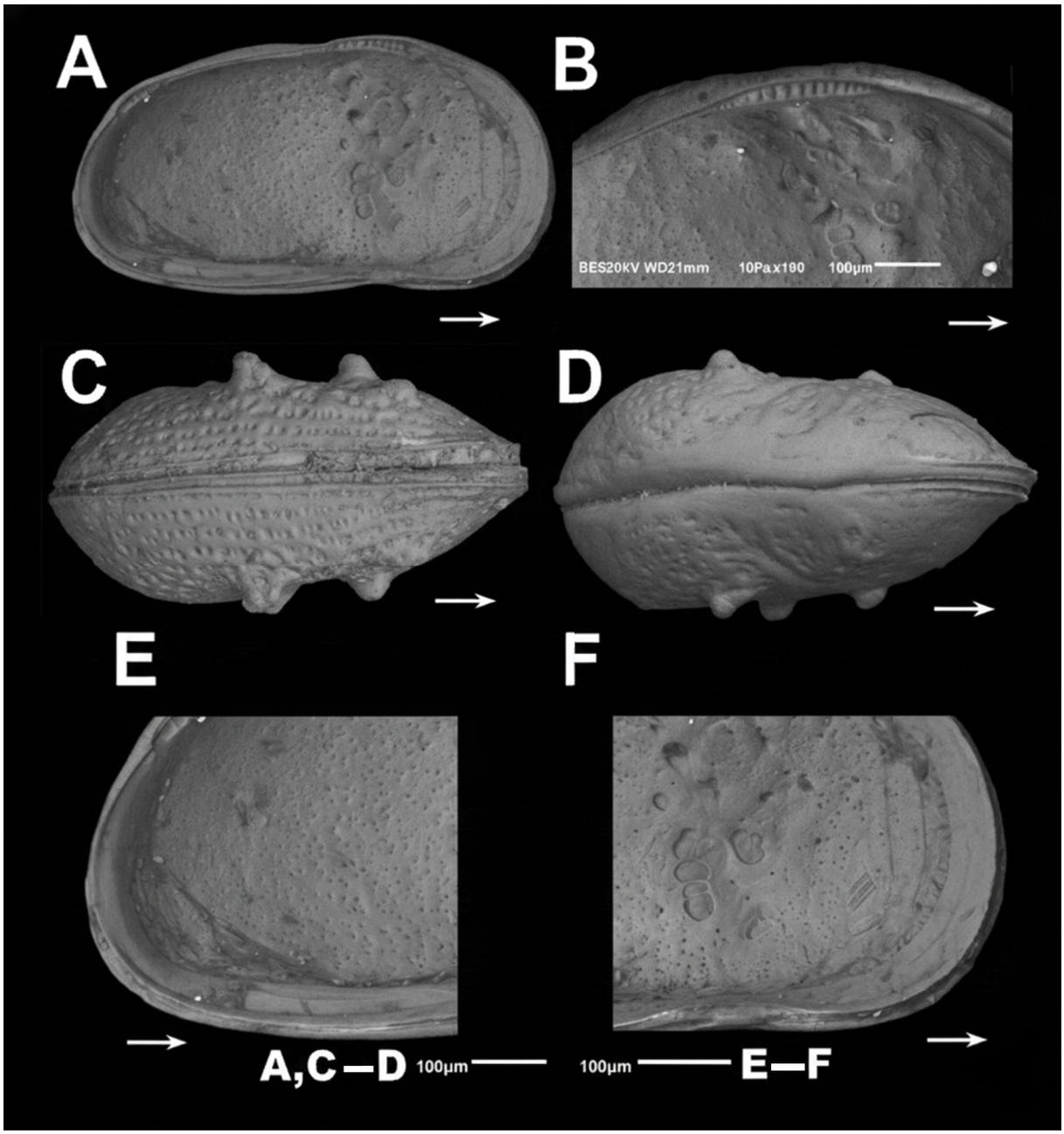


**Fig. 19.** *Cyprideis ichkabal* Macario-González & Cohuo sp. nov., holotype, ♂ (ECO-CH-Z-12542, ECO-CH-Z-12553) and paratype, ♀ (ECO-CH-Z-12553). **A**. Male left valve, internal view. **B**. Close-up of valve hinge anterior zone. **C**. Female carapace ventral view. **D**. Female carapace dorsal view. **E–F**. Close-up of male valve posterior and anterior margins, respectively. White arrows show the valve orientation toward the anterior margin.

L6 (Fig. 21B). Protopodite bears three strong, hairy setae. Second segment is hirsute, with one distal seta just exceeding the length of the following segment. Third segment is bare. Fourth segment bears one claw, three times as long as the segment that carries it.

L7 (Fig. 21C). Protopodite hirsute, with three strong, hairy setae. Second segment hirsute and carries one distal seta that exceeds the terminal segment. Third segment is bare. Fourth segment with one claw, 2.6 times as long as the segment that carries it.

Hemipenis (Fig. 21D). Triangular in shape, with an ovate base. DS is triangular and widened at the base. The DL is narrow and slightly curved medially. The Cp is hook-like. The CL is rounded and bears a small basal projection.

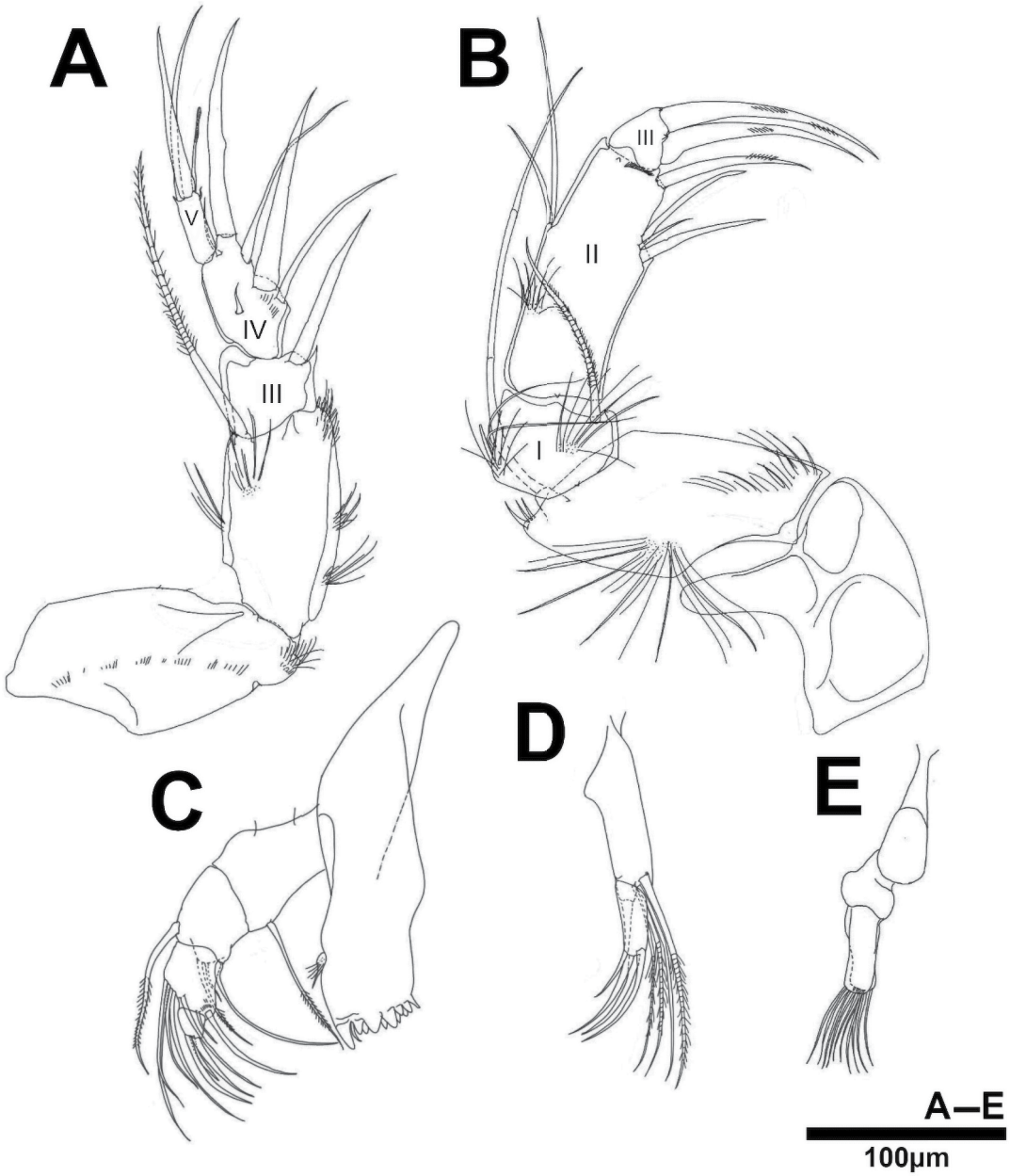


**Fig. 20.** *Cyprideis ichkabal* Macario-González & Cohuo sp. nov., holotype, ♂ (ECO-CH-Z-12542, ECO-CH-Z-12553). **A**. A1. **B**. A2. **C**. Md and Mdp. **D**. Mxlp. **E**. Brush-like organ.

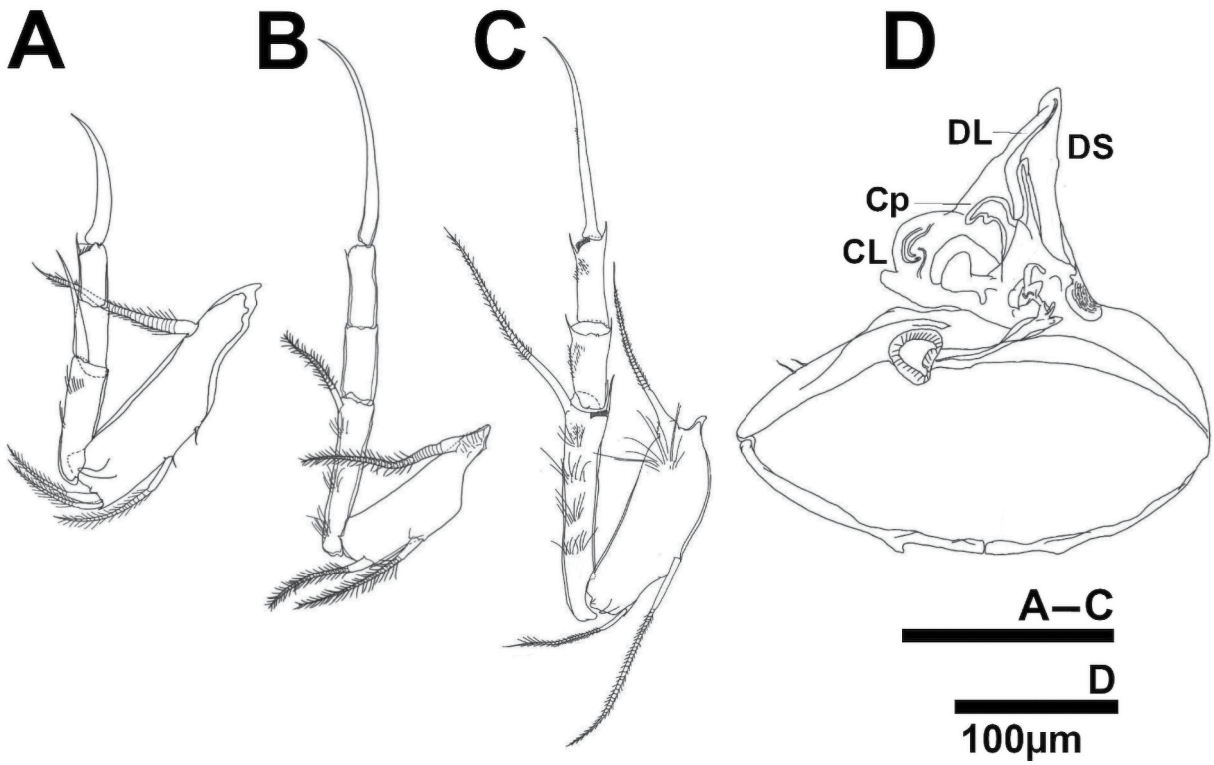


**Fig. 21.** *Cyprideis ichkabal* Macario-González & Cohuo sp. nov., holotype, ♂ (ECO-CH-Z-12542, ECO-CH-Z-12553). **A**. L5. **B**. L6. **C**. L7. **D**. Hemipenis.

**Female** (paratype)

Carapace. It is shorter but wider than in males. Valve surface pitted, with four to five nodes located from the anterior to the median region of the valves (Figs 18C–D, 19C–D). LV larger than RV anteriorly and posteriorly. RV (Fig. 18C) is 860.4 µm in length and 488.21 µm in height at the first third of the valve (greatest height). Inner lamella covers 10.8% anteriorly and 2.5% posteriorly (Fig. 18F). LV (Fig. 18D) measures 892.3 µm in length and 542.5 µm in height at the same position. Inner lamella covers 11.6% anteriorly and 3.5% posteriorly (Fig. 18E, G–H). Hinge as in males. In both valves, marginal pore canals are simple and bifurcated, located anteriorly, posteriorly, and ventrally.

A1 (Fig. 22A). 5-segmented. First, second, and third segments are as in males. Fourth segment (IV) bears four anteromedial setae, two of them claw-like and two additional short setae located medially in the segment. Fifth segment with one claw-like seta, one relatively long seta not reaching the tip of the claw, a very small seta, and one aesthetasc.

A2 (Fig. 22B). 5-segmented, slightly different from the male. Coxa and basis hirsute. Exopodite is represented by a large seta with two constrictions, extending beyond the end of the terminal segment. First (I) and second (II) endopodal segments are as in males, except for a posteromedial bundle of setae, where one claw-like seta is replaced by an aesthetasc. Third endopodal segment (III) bears two strong claws.

Md, Mdp and Mxlp. As in males.

L5 (Fig. 22C). Protopodite with three setae; dp seta not observed. Second segment with a strong distal seta. Third segment without a distinct seta; fourth segment bears a strong distal claw.

L6 (Fig. 22D). Protopodite with two strong, hairy setae; dp seta not observed. Second segment hirsute with a distal seta. Third segment is bare. Fourth segment carries a strong claw, 3.2 times as long as the segment that carries it.

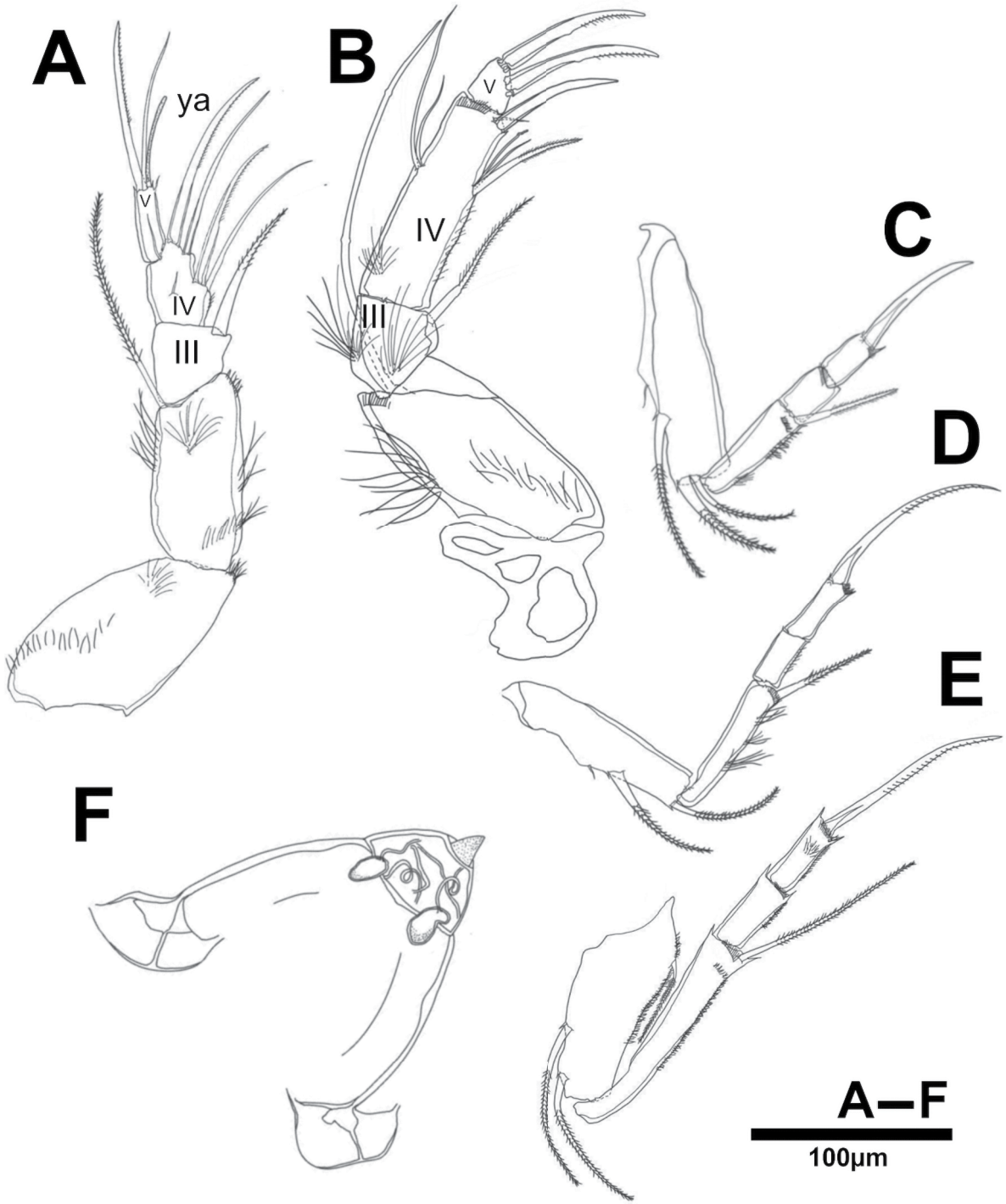


**Fig. 22.** *Cyprideis ichkabal* Macario-González & Cohuo sp. nov., paratype, ♀ (ECO-CH-Z-12543). **A**. A1. **B**. A2. **C**. L5. **D**. L6. **E**. L7. **F**. Sexual field.

L7(Fig. 22E). Protopodite hirsute, with three hairy setae. Second segment hirsute, bearing a distal seta that exceeds the terminal segment. Third segment without a visible seta. Fourth segment with a claw, 2.2 times as long as the segment that carries it.

Sexual field (Fig. 22F). Triangular, with two double-coiled ovaries ending distally in a small triangular caudal process.

**Differential diagnosis**

Of the 13 known *Cyprideis* species recorded from the Nearctic and Neotropical regions, *Cyprideis ichkabal* sp. nov. is morphologically most similar to *C. americana* (Sharpe, 1908) Sandberg & Plusquellec 1974, and *C. salebrosa* Van Den Bold, 1963, both of which are distributed in the Caribbean Sea. In comparison with *C. americana* (sensu Meyer *et al.* 2017), adult males are generally larger (1008–1120 μm) but have a similar height (498–589 μm) compared to *C. ichkabal* (940–990 μm in length and 480–520 μm height; n = 8). Valve outline also differs in females of *C. americana*, the dorsal margin displays an anterodorsal expansion that causes a steep slope toward the anterior margin. In contrast, in *C. ichkabal*, this region is more evenly rounded and lacks such an expansion (Fig. 18A). In males of *C. ichkabal*, the posterior region of the valve is mostly rounded (Fig. 18A), while it appears more downwardly projected in *C. americana*. Males of *Cyprideis salebrosa* (sensu Meyer *et al.* 2017) are remarkably larger (1034–1239 μm) than those of the new species. Additionally, the valve outline differs: *C. salebrosa* exhibits a convex ventral margin, whereas it is almost straight in *C. ichkabal* (Fig. 18 A–D). The posterior margin in *C. salebrosa* is slightly pointed, while it is rounded in the new species (Fig. 18A).

**Remarks**

The genus *Cyprideis* has a worldwide distribution and commonly inhabits marginal marine environments, where salinity can vary greatly, from freshwaters to hypersaline conditions. Due to this broad salinity range, species of *Cyprideis* are known to display phenotypic plasticity in traits such as valve size, surface reticulation, ornamentation, and nodation (Frenzel *et al.* 2012; Boomer *et al.* 2017; De Deckker & Lord 2017; Meyer *et al.* 2017). *Cyprideis torosa* (Jones, 1850) Jones 1857, for example, is recognized as a model species for paleo-salinity reconstruction, due to nodation patterns that vary in response to changes in salinity (Boomer & Frenzel 2011). *Cyprideis ichkabal* sp. nov. appears to be the only known species of *Cyprideis* currently distributed in a strictly freshwater environment. Average environmental variables at the sampling site: temperature 30.8°C, dissolved oxygen 4.84 mg $l^{-1}$, conductivity 3.21 mS $cm^{-1}$.

## Discussion

**Species assemblage in the freshwater Bacalar system and marine-estuarine species colonization**

The ostracode assemblage of the Bacalar system is diverse with 19 species. At least 15 of them display freshwater affinities as they are broadly distributed in low-elevation karstic plateaus of southern Mexico and northern Central America, such as *P. opesta*, *C. pelagica*, *S. intrepida*, and *H. putei* (Cohuo *et al.* 2018). The other four taxa demonstrated affinities to estuarine and marine waters, as other species from these genera have been observed almost exclusively in those environments worldwide.

Aquatic environments of the Bacalar system, despite similar environmental parameters such as water chemistry (Gondwe *et al.* 2010; Bauer-Gottwein *et al.* 2011; Perry *et al.* 2021), possess distinct geomorphological, hydrodynamic, and habitat characteristics that shape ostracode assemblages, similar to patterns observed in other zooplankton groups (Cervantes-Martínez *et al.* 2009; Tobon *et al.* 2018). Lake Bacalar is the most distinct water body in the system, with a species assemblage composed of fauna from the Yucatán karstic plateau and northern central America, alongside at least four species belonging to groups previously reported only from marine, estuarine, or anchialine environments: *Cyprideis* (Meyer

*et al.* 2017), *Thalassocypria* (Maddocks & Iliffe 1993), *Dolerocypria*, and *Perissocythere*. Species from these genera are known for their broad salinity tolerance and are occasionally found in low conductivity waters, but none have previously been recorded as native in freshwater ecosystems. Given their consistent presence in Bacalar, we considered these species as established residents. Nonetheless, their distribution in Bacalar represents an instance of marine or brackish-to-freshwater colonization. Such events are rare in zooplankton, as most marine species cannot overcome the osmotic and ionic barriers of freshwater habitats. Recent cases of marine zooplankton colonizing freshwater systems have been documented, such as the copepod *Eurytemora affinis* (Poppe, 1880), which has invaded freshwater environments multiple times over the past 200 years (Lee & Petersen 2002; Lee 2023). For the Bacalar ostracodes, we hypothesize that the high concentrations of dissolved carbonates and sulfates, reflected in conductivity values exceeding 2800 µS $cm^{-1}$, may facilitate osmotic regulation and allow marine species to adapt to freshwater conditions.

Intriguingly, other taxa with marine origins have been documented in the Bacalar system, including ichthyoplankton (Elías-Gutiérrez *et al.* 2018), amphipods, and even rays. The following non mutually exclusive mechanisms may explain these colonizations. First, passive transport via birds, reptiles or mammals crossing coastal habitats and freshwater environments. This may explain the introduction of smaller organisms but fails to account for the presence of large taxa such as rays. Second, marine water intrusion, at high marine water levels during the Pleistocene-Holocene or extreme hydrometeorological events such as hurricanes that may have caused regional-scale storm surges, introducing marine and estuarine waters (and species) into the freshwater system (for short or long term) and prompting ecological adaptation. For instance, in the late Pleistocene and early Holocene (Shaw 2016; Steele *et al.* 2023) high levels in the Caribbean Sea may have fully connected Bacalar with the nearby marine and estuarine environment, further leaving species isolated and facilitating adaptation. More recently, hurricane activity has shown to impact on coastal waters. Hurricane Janet, which impacted the study region in 1955, caused a marine intrusion extending 400 m inland at a depth of 3 m. Despite the fact that such events occur annually, the interaction between freshwater and marine systems during hurricanes remains poorly studied along the Caribbean coast (Martinez 2018; Alarcón 2019). Up to date, empirical data such as paleorecords from lake sediments, and indicators, such as salinity spikes, and shell deposition still lack, thus precluding an evaluation of these postulations. An alternative hypothesis is active dispersal by species with broad salinity tolerances moving upstream through low-energy systems such as the Hondo River. However, this fails to explain the absence of these marine-related species in the intermediate water bodies between Lake Bacalar and Chetumal Bay. Although all mechanisms remain likely, the presence of marine taxa in a freshwater system like Bacalar is unusual and merits further investigation.

**Conclusion**

The Bacalar hydrological system is a unique environment within the northern Neotropics, characterized by oligotrophic conditions, carbonate- and sulfate-rich waters, and a diverse and possible endemic ostracode fauna. In this study, we recorded a relatively high species richness (19 species) and formally described five new species. However, at least one additional species remains undescribed. *Thalassocypria zazilha* sp. nov., *Dolerocypria maanik* sp. nov., *Perissocythere cribrosa*, and *Cyprideis ichkabal* sp. nov. exhibit marine or estuarine affinities and were found in Bacalar alongside other marine-related taxa such as fishes, amphipods, and rays. To date, *T. zazilha*, *D. maanik*, and *C. ichkabal* are the only known representatives of their respective genera occurring long-term in freshwater environments.

This study represents the first description of the ostracode fauna in the Bacalar hydrological system. It documents not only species richness and taxonomic novelties, but also the first potential case of marine ostracode colonization of a freshwater system in this region. As such, it provides a baseline framework for the future use of ostracodes in bioindication and paleoenvironmental reconstructions in the northern

Neotropics, related to salinity changes, which may provide evidence for the dynamism of sea level rise and interaction with inland water ecosystems, and how it shapes the extant biota.

## Competing interests

This work was part of the project Tecnológico Nacional de México 26100.26-P. The authors have no competing interests to declare that are relevant to the content of this article.

## References

Alarcón M.N.R. 2019. El huracán Janet y el desastre de 1955 en Quintana Roo: estudio de una coyuntura crítica. *Antrópica, Revista de Ciencias Sociales y Humanidades* 5: 161–190. https://doi.org/10.32776/arcsh.v5i10.196

Bauer-Gottwein P., Gondwe B.R.N., Charvet G., Marín L.E., Rebolledo-Vieyra M. & Merediz-Alonso G. 2011. Review: The Yucatán Peninsula karst aquifer, Mexico. *Hydrogeology Journal* 19: 507–524. https://doi.org/10.1007/s10040-010-0699-5

Boomer I. & Frenzel P. 2011. Possible environmental and biological controls on carapace size in *Cyprideis torosa* (Jones, 1850). *Geologie und Paläontologie* 11: 26–27.

Boomer I., Frenzel P. & Feike M. 2017. Salinity-driven size variability in *Cyprideis torosa* (Ostracoda, Crustacea). *Journal of Micropalaeontology* 36: 63–69. https://doi.org/10.1144/jmpaleo2015-043

Broodbakker N.W. 1983. The subfamily Candoninae (Crustacea, Ostracoda) in the West Indies. *Bijdragen tot de Dierkunde* 53: 287–326. https://doi.org/10.1163/26660644-05302011

Broodbakker N.W. & Danielopol D.L. 1982. The chaetotaxy of Cypridacea (Crustacea, Ostracoda) limbs: proposals for a descriptive model. *Bijdragen tot de Dierkunde* 52: 103–120. https://doi.org/10.1163/26660644-05202003

Carrillo L., Yescas M., Nieto-Oropeza M.O., Elías-Gutiérrez M.J., Alcérreca-Huerta C., Palacios-Hernández E. & Reyes-Mendoza O.F. 2024. Investigating the morphometry and hydrometeorological variability of a fragile tropical karstic lake of the Yucatán Peninsula: Bacalar Lagoon. *Hydrology* 11: 68. https://doi.org/10.3390/hydrology11050068

Castro-Contreras S.I., Gingras M.K., Pecoits E., Aubet N.R., Petrash D., Castro-Contreras S.M., Dick G., Planavsky N. & Konhauser K.O. 2014. Textural and geochemical features of freshwater microbialites from Laguna Bacalar, Quintana Roo, Mexico. *PALAIOS* 29: 192–209. https://doi.org/10.2110/palo.2013.063

Cervantes-Martínez A., Mezeta-Barrera M. & Gutiérrez-Aguirre M.A. 2009. Limnología básica del lago cárstico turístico Cenote Azul en Quintana Roo, México. *Hidrobiológica* 19: 177–180.

Cohuo S., Macario-González L., Pérez L. & Schwalb A. 2017. Overview of Neotropical-Caribbean freshwater ostracode fauna (Crustacea, Ostracoda): identifying areas of endemism and assessing biogeographical affinities. *Hydrobiologia* 786: 5–21. https://doi.org/10.1007/s10750-016-2747-1

Cohuo S., Macario-González L., Pérez L., Sylvestre F., Paillès C., Curtis J.H., Kutterolf S., Wojewódka M., Zawisza, E., Szeroczyńska K. & Schwalb A. 2018. Climate ultrastructure and aquatic community response to Heinrich Stadials (HS5a-HS1) in the continental northern Neotropics. *Quaternary Science Reviews* 197: 75–91. https://doi.org/10.1016/j.quascirev.2018.07.015

Cohuo S., Moreno-López A., Escamilla-Tut N.Y., Pérez-Tapia A.M., Santos-Itzá I., Macario-González L.A., Villegas-Sánchez C.A. & Medina-Quej A. 2023. Assessment of water quality and heavy metal environmental risk on the peri-urban karst tropical lake La Sabana, Yucatán Peninsula. *Water* 15: 390. https://doi.org/10.3390/w15030390

Danielopol D.L. 1969. Recherches sur la morphologie de l'organe copulateur mâle chez quelques Ostracodes du genre *Candona* Baird (Fam. Cyprididae Baird). *In*: Neale J.W. (ed.) *The Taxonomy, Morphology and Ecology of Recent Ostracoda*: 136–153. Oliver and Boyd Ltd, Edinburgh.

Danielopol D.L. 1978. Über Herkunft und Morphologie der europäischen Süßwasser-Ostracoden. *Sitzungsberichte der österreichischen Akademie der Wissenschaften, mathematisch-naturwissenschaftliche Klasse, Abteilung I* 187: 1–162.

De Deckker P. & Lord A. 2017. *Cyprideis torosa*: a model organism for the Ostracoda? *Journal of Micropalaeontology* 36: 3–6. https://doi.org/10.1144/jmpaleo2016-100

de Jesús-Navarrete A. & Legorreta T.Á. 2022. Biological traits analysis of free-living nematodes as indicators of environmental quality at Lake Bacalar, Mexico. *Limnology* 23: 355–364. https://doi.org/10.1007/s10201-021-00693-9

de Jesús-Navarrete A., Yanez-Montalvo A., Falcón L.I. & Vargas-Espósitos A. 2021. Nematode fauna associated with freshwater microbialites in Bacalar Lake, Quintana Roo, Mexico. *Limnology* 22: 347–355. https://doi.org/10.1007/s10201-021-00662-2

Elías-Gutiérrez M., Kotov A.A. & Garfias-Espejo T. 2006. Cladocera (Crustacea: Ctenopoda, Anomopoda) from southern Mexico, Belize and northern Guatemala, with some biogeographical notes. *Zootaxa* 1119: 1–27. https://doi.org/10.11646/zootaxa.1119.1.1

Elías-Gutiérrez M., Valdez-Moreno M., Topan J., Young M.R. & Cohuo-Colli J.A. 2018. Improved protocols to accelerate the assembly of DNA barcode reference libraries for freshwater zooplankton. *Ecology and Evolution* 8: 3002–3018. https://doi.org/10.1002/ece3.3742

Frenzel P., Schulze I. & Pinto A. 2012. Noding of *Cyprideis torosa* valves (Ostracoda) – a proxy for salinity? New data from field observations and a long-term microcosm experiment. *International Review of Hydrobiology* 97: 314–329. https://doi.org/10.1002/iroh.201211494

Gamboa-Pérez H.C. & Schmitter-Soto J.J. 1999. Distribution of cichlid fishes in the littoral of Lake Bacalar, Yucatan Peninsula. *Environmental Biology of Fishes* 54: 35–43. https://doi.org/10.1023/A:1007443408776

Gischler E., Gibson M.A. & Oschmann W. 2008. Giant Holocene freshwater microbialites, Laguna Bacalar, Quintana Roo, Mexico. *Sedimentology* 55: 1293–1309. https://doi.org/10.1111/j.1365-3091.2007.00946.x

Gischler E., Golubic S., Gibson M.A., Oschmann W. & Hudson J.H. 2011. Microbial mats and microbialites in the freshwater Laguna Bacalar, Yucatan Peninsula, Mexico. *In*: Reitner J., Quéric N. & Arp G. (eds) *Advances in Stromatolite Geobiology*: 187–205. Springer, Berlin, Heidelberg. https://doi.org/10.1007/978-3-642-10415-2_13

Gondwe B.R.N., Lerer S., Stisen S., Marín L., Rebolledo-Vieyra M., Merediz-Alonso G. & Bauer-Gottwein P. 2010. Hydrogeology of the south-eastern Yucatan Peninsula: New insights from water level measurements, geochemistry, geophysics and remote sensing. *Journal of Hydrology* 389: 1–17. https://doi.org/10.1016/j.jhydrol.2010.04.044

Hamerlík L., Silva F.L. & Massaferro J. 2022. An illustrated guide of subfossil Chironomidae (Insecta: Diptera) from waterbodies of Central America and the Yucatan Peninsula. *Journal of Paleolimnology* 67: 201–258. https://doi.org/10.1007/s10933-021-00225-6

Horne D.J., Cohen A. & Martens K. 2002. Taxonomy, morphology and biology of Quaternary and living Ostracoda. *In*: *The Ostracoda: Applications in Quaternary Research*: 5–36. American Geophysical Union (AGU), EUA. https://doi.org/10.1029/131GM02

INEGI. National Institute of Statistics and Geography. 2020. Censo de Población y vivienda 2020. Available from https://www.inegi.org.mx/programas/ccpv/2020/ [accessed 17 Feb. 2025].

Johnson D.B., Beddows P.A., Flynn T.M. & Osburn M.R. 2018. Microbial diversity and biomarker analysis of modern freshwater microbialites from Laguna Bacalar, Mexico. *Geobiology* 16: 319–337. https://doi.org/10.1111/gbi.12283

Jones T.R. 1857. A monograph of the Tertiary Entomostraca of England. *Monographs of the Palaeontographical Society* 9: 1–68.

Karanovic I. 2012. *Recent Freshwater Ostracods of the World, Crustacea, Ostracoda, Podocopida*: 618. Springer, Berlin.

Keyser D. 1975. Ostracoden aus den Mangrovegebieten von Südwest-Florida (Crustacea: Ostracoda, Podocopa). *Abhandlungen und Verhandlungen des Naturwissenschaftlichen Vereins in Hamburg* 18/19: 255–290.

Lee C.E. 2023. Genome architecture underlying salinity adaptation in the invasive copepod *Eurytemora affinis* species complex: A review. *iScience* 26: 107851. https://doi.org/10.1016/j.isci.2023.107851

Lee C.E. & Petersen C.H. 2002. Genotype-by-environment interaction for salinity tolerance in the freshwater-invading copepod *Eurytemora affinis*. *Physiological and Biochemical Zoology* 75: 335–344. https://doi.org/10.1086/343138

Macario-González L., Cohuo S., Elías-Gutiérrez M., Vences M., Pérez L. & Schwalb A. 2018. Integrative taxonomy of freshwater ostracodes (Crustacea: Ostracoda) of the Yucatán Peninsula, implications for paleoenvironmental reconstructions in the northern Neotropical region. *Zoologischer Anzeiger* 275: 20–36. https://doi.org/10.1016/j.jcz.2018.04.002

Macario-González L., Cohuo S., Angyal D., Pérez L. & Mascaró M. 2021. Subterranean waters of Yucatán Peninsula, Mexico, reveal epigean species dominance and intraspecific variability in freshwater ostracodes (Crustacea: Ostracoda). *Diversity* 13: 44. https://doi.org/10.3390/d13020044

Macario-González L., Cohuo S., Hoelzmann P., Pérez L., Elías-Gutiérrez M., Caballero M., Oliva A., Palmieri M., Álvarez M.R. & Schwalb A. 2022. Geodiversity influences limnological conditions and freshwater ostracode species distributions across broad spatial scales in the northern Neotropics. *Biogeosciences* 19: 5167–5185. https://doi.org/10.5194/bg-19-5167-2022

Machain-Castillo M.L. & Gío-Argáez R. 1993. Diversidad de ostrácodos de los mares mexicanos. *Revista de la Sociedad Mexicana de Historia Natural* 44: 251–266.

Maddocks R.F. & Iliffe T.M. 1993. Thalassocypridine Ostracoda from anchialine habitats of Jamaica. *Journal of Crustacean Biology* 13: 142–164. https://doi.org/10.1163/193724093X00525

Martens K. 1987. Homology and functional morphology of the sexual dimorphism in the antenna of *Sclerocypris* Sars, 1924 (Crustacea, Ostracoda, Megalocypridinae). *Bijdragen tot de Dierkunde* 57: 183–190. https://doi.org/10.1163/26660644-05702003

Martens K. 1990. Taxonomic revision of African Cypridini. Part I: the genera *Cypris* O.F. Müller, *Pseudocypris* Daday and *Globocypris* Klie (Crustacea, Ostracoda). *Bulletin de l'Institut royal des Sciences naturelles de Belgique, Biologie* 60: 127–172.

Martinez F.O. 2018. Turismo oscuro: el desastre del huracán Janet de 1955 en la ciudad de Chetumal, México. *Teoría y Praxis* 24: 175–196.

Meisch C. 2000. Freshwater Ostracoda of Western and Central Europe. *In*: Schwoerbel J. & Zwick P. (eds) *Süßwasserfauna von Mitteleuropa*. Spektrum Akademischer Verlag, Heidelberg, Berlin.

Meisch C., Smith R.J. & Martens K. 2019. A subjective global checklist of the extant non-marine Ostracoda (Crustacea). *European Journal of Taxonomy* 492: 1–135. https://doi.org/10.5852/ejt.2019.492

Meisch C., Smith R.J. & Martens, K. (2024). An updated subjective global checklist of the extant non-marine Ostracoda (Crustacea). *European Journal of Taxonomy* 974 (1): 1–144. https://doi.org/10.5852/ejt.2024.974.2767

Mercado-Salas N.F., Khodami S. & Martínez P. 2021. Copepods and ostracods associated with bromeliads in the Yucatán Peninsula, Mexico. *PLoS ONE* 16 (3): e0248863. https://doi.org/10.1371/journal.pone.0248863

Mesquita-Joanes F., Aguilar-Alberola J.A., Palero F. & Rueda J. 2020. A new species of *Cypris* (Crustacea: Ostracoda) from the Iberian Peninsula and the Balearic Islands, with comments on the first ostracod named using the Linnean system. *Zootaxa* 4759 (1): 113–131. https://doi.org/10.11646/zootaxa.4759.1.8

Meyer J., Wrozyna C., Gross M., Leis A. & Piller W.E. 2017. Morphological and geochemical variations of *Cyprideis* (Ostracoda) from modern waters of the northern Neotropics. *Limnology* 18: 251–273. https://doi.org/10.1007/s10201-016-0504-9

Montes-Ortiz L. & Elias-Gutierrez M. 2018. Faunistic survey of the zooplankton community in an oligotrophic sinkhole, Cenote Azul (Quintana Roo, Mexico), using different sampling methods, and documented with DNA barcodes: Zooplankton baseline in a karstic system. *Journal of Limnology* 77 (3): 428–440. https://doi.org/10.4081/jlimnol.2018.1746

Montes-Ortiz L. & Elías-Gutiérrez M. 2020. Water mite diversity (Acariformes: Prostigmata: Parasitengonina: Hydrachnidiae) from karst ecosystems in southern of [sic] Mexico: A barcoding approach. *Diversity* 12: 329. https://doi.org/10.3390/d12090329

Neale J.W. 1976. On *Cypris decaryi* Gauthier. *Stereo-Atlas of Ostracod Shells* 3 (23): 133–140.

Ochoa S.A.H., Navarro-Martínez A., Ellis E.A. & Gómez I.U.H. 2022. Deforestación en el municipio de Bacalar, Quintana Roo, México durante el período 1993-2017. *Madera y Bosques* 28: e2832396. https://doi.org/10.21829/myb.2022.2832396

Perry E., Velazquez-Oliman G. & Marin L. 2002. The hydrogeochemistry of the karst aquifer system of the northern Yucatan Peninsula, Mexico. *International Geology Review* 44: 191–221. https://doi.org/10.2747/0020-6814.44.3.191

Perry E., Paytan A., Pedersen B. & Velazquez-Oliman G. 2009. Groundwater geochemistry of the Yucatan Peninsula, Mexico: Constraints on stratigraphy and hydrogeology. *Journal of Hydrology* 367: 27–40. https://doi.org/10.1016/j.jhydrol.2008.12.026

Perry E.C., Leal-Bautista R.M., Velázquez-Olimán G., Sánchez-Sánchez J.A. & Wagner N. 2021. Aspects of the hydrogeology of southern Campeche and Quintana Roo, Mexico. *Boletín de la Sociedad Geológica Mexicana* 73: A011020. https://doi.org/10.18268/bsgm2021v73n1a011020

Poppe S.A. 1880. Über eine neue Art der calaniden Gattung *Temora* Baird. *Abhandlungen des naturwissenschaftlichen Vereins* 7: 55–60.

Rosa J., Martens K. & Higuti J. 2023. Dried aquatic macrophytes are floating egg banks and potential dispersal vectors of ostracods (Crustacea) from pleuston communities. *Hydrobiologia* 850: 1319–1329. https://doi.org/10.1007/s10750-022-04818-8

Sharpe R.W. 1908. A further report on the Ostracoda of the United States National Museum. *Proceedings of the United States National Museum* 35: 399–430. https://doi.org/10.5479/si.00963801.35-1651.399

Shaw C.E. 2016. Late Pleistocene bays and reefs: Ancestors to the modern Caribbean Coast, Yucatan Peninsula, Mexico. *Journal of Coastal Research* 32 (2): 280–285. https://doi.org/10.2112/JCOASTRES-D-14-00083.1

Sandberg P.A. & Plusquellec P.L. 1974. Notes on the anatomy and passive dispersal of *Cyprideis* (Cytheracea, Ostracoda). *Geoscience and Man* 6: 1 –26.

Steele R.E., Reinhardt E.G., Devos F., Meacham S., LeMaillot C., Gabriel J.J., Rissolo D., Vera C.A., Peros M.C., Kim S., Marshall M. & Zhu J. 2023. Evidence of recent sea-level rise and the formation of a classic Maya canal system inferred from Boca Paila cave sediments, Sian Ka'an biosphere, Mexico. *Quaternary Science Reviews* 31: e108117. https://doi.org/10.1016/j.quascirev.2023.108117

Tobon N.I., Rebolledo M., Paytan A., Broach K.H., Hernández L.M., Velázquez N.I.T., Vieyra M.R., Paytan A., Broach K.H. & Terrones L.M.H. 2018. Hydrochemistry and carbonate sediment characterization of Bacalar Lagoon, Mexican Caribbean. *Marine and Freshwater Research* 70: 382–394. https://doi.org/10.1071/MF18035

Tomowski M., Kiemel K., Birnbach T., Parry V., Ristow M., Roeleke M., Tiedemann R., Weithoff G. & Jeltsch F. 2025. A dual role of common mammals as dispersers of plants and micro-invertebrates across isolated wetlands. *Diversity and Distributions* 31 (9): e70088. https://doi.org/10.1111/ddi.70088

Uh-Navarrete A.E., Valdez-Moreno M., Callejas-Jiménez M.E. & Vásquez-Yeomans L. 2023. Discovering the fish fauna of a lagoon from the southeast of the Yucatan Peninsula, Mexico, using DNA barcodes. *PeerJ* 11: e16285. https://doi.org/10.7717/peerj.16285

Valdez-Moreno M., Ivanova N.V., Elías-Gutiérrez M., Pedersen S.L., Bessonov K. & Hebert P.D.N. 2019. Using eDNA to biomonitor the fish community in a tropical oligotrophic lake. *PLoS ONE* 14: e0215505. https://doi.org/10.1371/journal.pone.0215505

Vinogradova E.M. 2008. Six new species of *Polypedilum* Kieffer, 1912 from the Yucatán peninsula. *Spixiana* 31: 277–288.

Yanez-Montalvo A., Gómez-Acata S., Águila B., Hernández-Arana H. & Falcón L.I. 2020. The microbiome of modern microbialites in Bacalar Lagoon, Mexico. *PLoS ONE* 15: e0230071. https://doi.org/10.1371/journal.pone.0230071

Printed versions of all papers are deposited in the libraries of two of the institutes that are members of the *EJT* consortium: Muséum national d'Histoire naturelle, Paris, France and Royal Museum for Central Africa, Tervuren, Belgium. The other members of the consortium are: Royal Belgian Institute of Natural Sciences, Brussels, Belgium; Meise Botanic Garden, Meise, Belgium; Natural History Museum of Denmark, Copenhagen, Denmark; Naturalis Biodiversity Center, Leiden, the Netherlands; Museo Nacional de Ciencias Naturales-CSIC, Madrid, Spain; Leibniz Institute for the Analysis of Biodiversity Change, Bonn – Hamburg, Germany; National Museum of the Czech Republic, Prague, Czech Republic; The Steinhardt Museum of Natural History, Tel Aviv, Israël.

## Appendix 1

Sampling sites geographical location and ostracode assemblages in lakes of the Bacalar hydrological system during the period 2010–2021.

| Lake | Latitude | Longitude | Date | Ostracode assemblage |
|---|---|---|---|---|
| Bacalar 1 | 18.64′0314″ N | 88.40′8149″ W | 2010 | *C. pelagica*, *T. zazilha* sp. nov., *D. maanik* sp. nov., *P. opesta*, *H. putei*, *C. vidua*, *A. yucatanensis*, *C. gibbera*, *S. intrepida*, *P. tzabek* sp. nov., *C. ichkabal* sp. nov., *Cypria* sp. |
| Bacalar 2 | 18.65′9122″ N | 88.39′602″ W | | |
| Bacalar 3 | 18.67′6295″ N | 88.38′5171″ W | | |
| Bacalar 4 | 18.73′2383″ N | 88.34′6843″ W | | |
| Bacalar 5 | 18.74′3974″ N | 88.32′6089″ W | | |
| Bacalar 6 | 18.84′8283″ N | 88.25′3618″ W | | |
| Bacalar 7 | 18.87′7243″ N | 88.23′5088″ W | | |
| Bacalar 8 | 18.65′9122″ N | 88.39′602″ W | 2013 | *C. pelagica*, *T. zazilha* sp. nov., *D. maanik* sp. nov., *P. opesta*, *H. putei*, *C. vidua*, *V. pagliolii*, *C. unispinosa*, *C. gibbera*, *Cypria* sp. |
| Bacalar 9 | 18.67′6295″ N | 88.38′5171″ W | | |
| Bacalar 10 | 18.73′2383″ N | 88.34′6843″ W | | |
| Bacalar 11 | 18.87′7116″ N | 88.23′4683″ W | | |
| Bacalar 12 | 18.65′9122″ N | 88.39′602″ W | 2015 | *C. pelagica*, *T. zazilha* sp. nov., *P. opesta*, *H. putei*, *C. vidua*, *A. yucatanensis*, *V. pagliolii*,*C. ilosvayi*, *C. gibbera*, *S. intrepida*, *P*. cf. *cribrosa*, *P. tzabek* sp. nov., *Cypria* sp. |
| Bacalar 13 | 18.67′6295″ N | 88.38′5171″ W | | |
| Bacalar 14 | 18.73′2383″ N | 88.34′6843″ W | | |
| Bacalar 15 | 18.87′7116″ N | 88.23′4683″ W | | |
| Bacalar 16 | 18.64′0314″ N | 88.40′8149″ W | 2019 | *C. pelagica*, *T. zazilha* sp. nov., *D. maanik* sp. nov., *P. opesta*, *H. putei*, *C. vidua*, *P*. cf. *cribrosa*, *A. yucatanensis*, *C. ilosvayi*, *D. stevensoni*, *P. tzabek* sp. nov., *C. ichkabal* sp. nov. |
| Bacalar 17 | 18.65′9122″ N | 88.39′602″ W | | |
| Bacalar 18 | 18.73′2383″ N | 88.34′6843″ W | | |
| Bacalar 19 | 18.74′3974″ N | 88.32′6089″ W | | |
| Bacalar 20 | 18.87′5535″ N | 88.23′5593″ W | | |
| Bacalar 21 | 18.64′0314″ N | 88.40′8149″ W | 2022 | *C. pelagica*, *T. zazilha* sp. nov., P. *opesta*, *H. putei*, *C. vidua*, *A. yucatanensis*, *V. pagliolii*,*C. ilosvayi*, *C. gibbera*, *S. intrepida*, *P.* cf. *cribrosa*, *P. tzabek* sp. nov., C. *ichkabal* sp. nov. |
| Bacalar 22 | 18.65′9122″ N | 88.39′602″ W | | |
| Bacalar 23 | 18.67′6416″ N | 88.38′515″ W | | |
| Bacalar 24 | 18.71′1961″ N | 88.37′8443″ W | | |
| Bacalar 25 | 18.73′2383″ N | 88.34′6843″ W | | |
| Bacalar 26 | 18.87′7116″ N | 88.23′4683″ W | | |
| Milagros 1 | 18.51′393″ N | 88.42′9227″ W | 2010 | *C. pelagica*, *T. zazilha* sp. nov., *D. maanik* sp. nov., *P. opesta*, *C. vidua*, *C. ilosvayi*, *P. tzabek* sp. nov. |
| Milagros 2 | 18.51′4866″ N | 88.42′2255″ W | | |
| Milagros 3 | 18.51′3211″ N | 88.41′2673″ W | | |
| Milagros 4 | 18.51′393″ N | 88.42′9227″ W | 2013, 2015 | *C. pelagica*, *T. zazilha* sp. nov., *P. opesta*, *C. ilosvayi* |
| Milagros 5 | 18.51′4866″ N | 88.42′2255″ W | | |
| Milagros 6 | 18.51′3211″ N | 88.41′2673″ W | | |
| Milagros 7 | 18.51′4259″ N | 88.42′6254″ W | 2019 | *C. pelagica*, *D. maanik* sp. nov., *C. vidua*, *V. pagliolii* |
| Milagros 8 | 18.51′7235″ N | 88.40′753″ W | | |
| Milagros 9 | 18.51′0176″ N | 88.41′6301″ W | | |
| Milagros 10 | 18.50′1229″ N | 88.43′2283″ W | | |

| Lake | Latitude | Longitude | Date | Ostracode assemblage |
|---|---|---|---|---|
| Milagros 11 | 18.51′4259″ N | 88.42′6254″ W | 2022 | *C. pelagica*, *P. opesta*, *D. maanik* sp. nov., *C. vidua*, *A. yucatanensis*, *C. ilosvayi*, *P. tzabek* sp. nov. |
| Milagros 12 | 18.51′7235″ N | 88.40′753″ W | | |
| Milagros 13 | 18.51′0176″ N | 88.41′6301″ W | | |
| Milagros 14 | 18.50′1229″ N | 88.43′2283″ W | | |
| Xul-ha 1 | 18.54′5777″ N | 88.46′1153″ W | 2010 | *P. opesta*, *C. vidua*, *C. ilosvayi*, *Cypria* sp., *D. stevensonii* |
| Xul ha 2 | 18.55′52901″ N | 88.45′8671″ W | | |
| Xul-ha 3 | 18.55′9394″ N | 88.44′7186″ W | | |
| Xul ha 4 | 18.54′5777″ N | 88.46′1153″ W | 2013 | *C. pelagica*, *P. opesta*, *H. putei*, *C. vidua* |
| Xul-ha 5 | 18.55′52901″ N | 88.45′8671″ W | | |
| Xul-ha 6 | 18.55′9394″ N | 88.44′7186″ W | | |
| Xul-ha 7 | 18.54′8978″ N | 88.46′077″ W | 2015 | *C. pelagica*, *H. putei*, *C. gibbera*, *P. tzabek* sp. nov., *Cypria* sp. |
| Xul-ha 8 | 18.55′5187″ N | 88.45′6903″ W | | |
| Xul-ha 9 | 18.54′659″ N | 88.45′6975″ W | | |
| Xul-ha 10 | 18.54′8978″ N | 88.46′077″ W | 2019 | *C. pelagica*, *T. zazilha* sp. nov., *P. opesta*, *C. vidua*, *C. gibbera*, *Cypria* sp. |
| Xul-ha 11 | 18.55′5187″ N | 88.45′6903″ W | | |
| Xul-ha 12 | 18.54′659″ N | 88.45′6975″ W | | |
| Xul-ha 13 | 18.54′7679″ N | 88.46′0137″ W | 2022 | *T. zazilha* sp. nov., *P. opesta*, *H. putei*, *C. vidua*, *P. tzabek* sp. nov. |
| Xul-ha 14 | 18.55′3016″ N | 88.45′6571″ W | | |
| Xul-ha 15 | 18.55′812″ N | 88.44′9171″ W | | |
| Xul-ha 16 | 18.54′9578″ N | 88.45′5388″ W | | |
| Estero Chac1 | 18.57′7835″ N | 88.41′9003″ W | 2010, 2013, 2015, 2019, 2022 | *T. zazilha* sp. nov., *P. opesta*, *H. putei*, *C. vidua*, *C. ilosvayi*, *C. gibbera*, *P. tzabek* sp. nov., *Cypria* sp. |
| Estero Chac2 | 18.52′8714″ N | 88.42′9189″ W | | |
| Estero Chac3 | 18.51′7883″ N | 88.43′7989″ W | | |
| La Sabana 1 | 18.54′6502″ N | 88.31′3584″ W | 2010, 2013, 2022 | *C. pelagica*, *C. vidua* |
| La Sabana 2 | 18.54′1302″ N | 88.31′691″ W | | |
| La Sabana 3 | 18.53′3975″ N | 88.32′5182″ W | | |
| La Sabana 4 | 18.52′9231″ N | 88.32′7912″ W | | |
| La Sabana 5 | 18.52′5053″ N | 88.33′7891″ W | | |
| La Sabana 6 | 18.51′6821″ N | 88.51′6821″ W | | |
| La Sabana 7 | 18.51′6656″ N | 88.34′8923″ W | | |
| Wetlands1 | 18.51′9424″ N | 88.43′9826″ W | 2010, 2013, 2015, 2022 | *C. pelagica*, *P. opesta*, *C. vidua*, *V. pagliolii*, *C. ilosvayi*, *P. tzabec* sp. nov., *Cypria* sp., *C. unispinosa* |
| Wetlands2 | 18.51′3267″ N | 88.44′8773″ W | | |
| Wetlands3 | 18.53′0691″ N | 88.37′852″ W | | |
| Wetlands4 | 18.63′07″ N | 88.41′1527″ W | | |
| Wetlands5 | 18.74′642″ N | 88.32′5649″ W | | |
| Pond 1 | 18.51′5441″ N | 88.35′1181″ W | 2022 | *C. nicte* sp. nov. |
| Pond 2 | 18.52′1498″ N | 88.42′7956″ W | 2022 | *S. major* |

## Appendix 2

Average environmental parameters in sampling lakes in the Bacalar hydrological system.

| **Sampled lakes** | **Temperature °C** | **Dissolved oxygen mg $l^{-1}$** | **pH** | **Conductivity µS $cm^{-1}$** | **Depth m** |
|---|---|---|---|---|---|
| Bacalar | 30.2 | 7.3 | 8 | 2100 | 0.4 |
| Milagros | 27.9 | 7.9 | 8.1 | 2700 | 0.5 |
| Xul Ha | 30.2 | 8.2 | 7.9 | 2000 | 0.5 |
| La Sabana | 31 | 7.4 | 9.5 | 2110 | 0.8 |
| Estero Chac | 30.4 | 7.7 | 8.5 | 2200 | 0.9 |
| Pond 1 | 32 | 7.1 | 8.5 | 1006 | 0.6 |
| Pond 2 | 30 | 6.3 | 7.8 | 1200 | 0.5 |
| wetlands | 32.4 | 5.3 | 7.4 | 1100 | 0.3 |